Journal of African Earth Sciences 196 (2022) 104697

Contents lists available at ScienceDirect

Journal of African Earth Sciences

journal homepage: www.elsevier.com/locate/jafrearsci

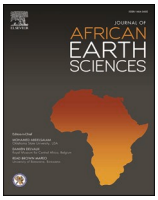

# Karstic geomorphology of carbonate Ouarsenis Piedmont (Boukadir region, Chelif) in Algeria: The role of the Messinian Salinity Crisis

Meriem L. Moulana [a,b,*], Aurélia Hubert-Ferrari [a], Mostefa Guendouz [b], Sébastien Doutreloup [c], Sarah Robinet [a], Bernard Collignon [d], Camille Ek [e]

[a] Department of Geography, University of Liege, Clos Mercator 3, 4000, Liege, Belgium
[b] Faculty of Earth Sciences, Geographical and Territorial Planning, University of Science and Technology Houari Boumediene, (USTHB), El Alia, BP 32, Bab Ezzouar, 16111, Algiers, Algeria
[c] Laboratory of Climatology, Département of Geography, UR SPHERES, University of Liège, 4000, Liège, Belgium
[d] Hydroconseil, 198, chemin d'Avignon, 84 470, Chateauneuf de Gadagne, France
[e] Department of Geology, University of Liège, 4000, Liège, Belgium

ARTICLE INFO

*Keywords:*
Karst
Messinian
Sinkholes
Mediterranean
Carbonate

ABSTRACT

Algeria displays various karst landscapes due to its diversity in lithology, relief, age and climate. On 16th June 1988, in the northwest of Algeria, a 60 m wide sudden collapse occurred in the Chelif Basin about 1 km north of a marginal carbonate platform. Despite this large event and visible karst dissolutions in the platform, this region has not been classified among the karst areas of Algeria yet. Our study focuses on this Messinian carbonates that form the northern piedmont of the Ouarsenis Mountain range and are covered to the north by Plio-Quaternary deposits. The geological and geomorphological data that we collected reveal that the present-day karstification is limited at the outcropping surface. Present-day carbonate dissolution is impeded by the absence of a topsoil supplying $CO_2$ and by the presence of a calcrete improving the drainage. Although dissolution at depth is generally diffuse due to the porous and friable nature of the carbonates, two factors can, on the contrary, concentrate water infiltration: the presence of a network of more or less subvertical fractures and, occasionally, at the surface, the absence of calcrete, independently of the fracturing nodes There are few ponors and sinkholes present. The endokarst is still present as evidenced by rare caves. In epikarst, solution pipes and shelter caves are prevalent. The later results from differential weathering in relation with the carbonate facies and the progressive calcrete cementation in valleys and slopes during river incision. Near valley bottom, shelters are arranged in steps like terraces. This morphology is related to base-level lowering in relation with the deformation and uplift of the Ouarsenis piedmont. Near the southern edge of the Chelif Basin, deep (>55m) karstic voids are present and associated with paleo-valley incision presently burried by Plio-Quaternary deposits. We interpreted the large 1988 collapse in relation with this paleokarst and propose that its triggering was partly induced by a lowering of the aquifers due to a deficit of precipitation. The deep paleokarst formation and the buried river incision are attributed to the low base-level during the Messinian Salinity Crisis (5.97–5.33 Ma). We evidenced an upper karstic dissolution level filled that is attributed to a per ascendum evolution of the karstic phreatic network in relation with the following Pliocene aggradation.

## 1. Introduction

Karst development is strongly influenced by climate and relief (*Woodward and Lewin, 2009*). These natural parameters display large variations in Algeria (*Collignon, 1991*, *2022*). Another most important parameter is the lithology and the carbonate formations in Algeria cover a variety of geological times from the Carboniferous, Triassic, Jurassic, Cretaceous to the Miocene post-nappe (*Collignon, 1991*; *Moulana, 2022*) (Fig. 1). .

The geoscientific litterature about karst landscapes in Algeria is restricted, though their study is important for at least two main reasons. First, karstic terrains are often the main useable aquifer formation in Algeria like in other Mediterranean countries (*Hamed* et al. *2018*; *Nekkoub* et al. *2020*; *Besser* et al. *2021*). Indeed, these terrains represent

* Corresponding author. Department of Geography, University of Liege, Clos Mercator 3, 4000, Liege, Belgium.
*E-mail address:* ml.moulana@uliege.be (M.L. Moulana).

https://doi.org/10.1016/j.jafrearsci.2022.104697
Received 8 January 2022; Received in revised form 12 August 2022; Accepted 12 August 2022
Available online 23 August 2022
1464-343X/

strategic water reserves, which are a crucial issue for populations and farming, as in the study area (*Bakalowicz, 2018*; *Brahmi* et al. *2021*). Superficial and underground drainage networks are connected, and their study is important to prevent pollution (*Hamad* et al. *2021*; *Ncibi* et al. *2021*). Water is poorly filtered in karstic rocks due to their high fracture permeability. Thus, the risk of water contamination is important (*Ek* et al., *1999*). Second, karst areas represent a collapse risk, thus creating a serious human and socio-economic damage (*Mouici* et al. *2017*). Karst can thus induce important constraints in land management (*Ek* et al., *1997*).

This study focuses on the marginal Messinian carbonate platform in the northern piedmont of the Ouarsenis mountains that has been only recently classified among the karstic areas of Algeria yet (*Moulana* et al., *2021*). It is located in the Boukadir region on the southern edge of the 20 km wide lower Chelif basin crossed by the Chelif River (Fig. 2). There is a lack of knowledge in karst geomorphology about this carbonate platform even if there is a large collapse sinkhole called Bir Djeneb or « le puits du Diable » (Birebent, 1947a). In addition, on 16$^{th}$ June 1988, a huge collapse pit occurred about 1 km north of the platform, in the Chelif Basin (*Ourabia and Benallal, 1989*). It broke the national road RN4 that connects the capital Algiers to the city of Oran in the west. Thus, the study aims to unravel processes that lead to the formation of deep shafts in the area, the climatic conditions in 1988, a potential trigger of the collapse pit, and more generally to provide new insight regarding the karstification of the area in relation with faulting and base-level changes.

## 2. General seeting

The study area comprises the Ouarsenis piedmont to the south and the Chelif Basin to the north. The Ouarsenis piedmont is composed of 3 main geological units. The basal up to 500 m thick Tortonian to Messinian blue marls (blue in Fig. 3-A) are overlain by two Messinian bioclastic carbonate units (grouped in orange in Fig. 3-A) with low dips (*Neurdin- Trescartes, 1992*; *Moulana et al., 2021*). The lower bioclastic carbonate unit is ~70 m thick and the upper lithothamnium carbonate unit is ~80 m thick. The top of the carbonate platform forms the piedmont of the Ouarsenis mountains. The 1988 large shaft that opened in the middle of National 4 highway between Oued Sly and Boukadir, is located 1.5 km north of the outcropping carbonate piedmont in the Chelif Basin. It is filled with Cenozoic marine and continental sediments that started to be deposited during the Langhian and Serravalian. The most recent sediments comprise thick Quaternary alluvium deposited by the Chelif River (Fig. 3-A) above continental Pliocene (Villafranchian) and marine Pliocene (Plaisancian-Astian) outcropping north and northeast of the Chelif Basin. This Basin is presently occupied by the Chelif River that runs from north-east to south-west. Its tributaries from the Ouarsenis Range runs from the south to the north, the main ones in the study area being from West to East, Oued Rhiou, Oued Touchait, Oued Taflout and Oued Sly (Fig. 3).

The Chelif Basin is also part of the Tellian atlas domain where compressional tectonic structures are predominant (*Meghraoui, 1988*; *Meghraoui* et al., *1996*; *Yelles-Chaouche* et al., *2006*; *Aifa and Zaagane, 2015*). This region is characterized by shallow seismicity and active faulting (*Beldjoudi* et al., *2012*). In the study area, geological formations are cut by the Relizane left lateral strike slip fault and the Boukadir thrust fault (Fig. 3) (*Meghraoui, 1988*; *Meghraoui* et al., *1996*). The Boukadir thrust crosses the Chelif Basin and ends near the Relizane Fault at the base of the Ouarsenis Piedmont. It strikes N50°E and bounds the Boukadir anticlinal structure (Fig. 3). In the Chelif Basin, this structure forms at the surface the El Kherba hill along which continental Pliocene siltstones, sandstones and conglomerates crop out as well as older Marine Pliocene sandstone on its southern edge (*Moulana* et al., *2021*).

The study area is also characterized by a semi-arid continental type of climate famous for its harshness, despite the proximity of the sea, with very hot and clear summers and long, chilly and partly cloudy winters

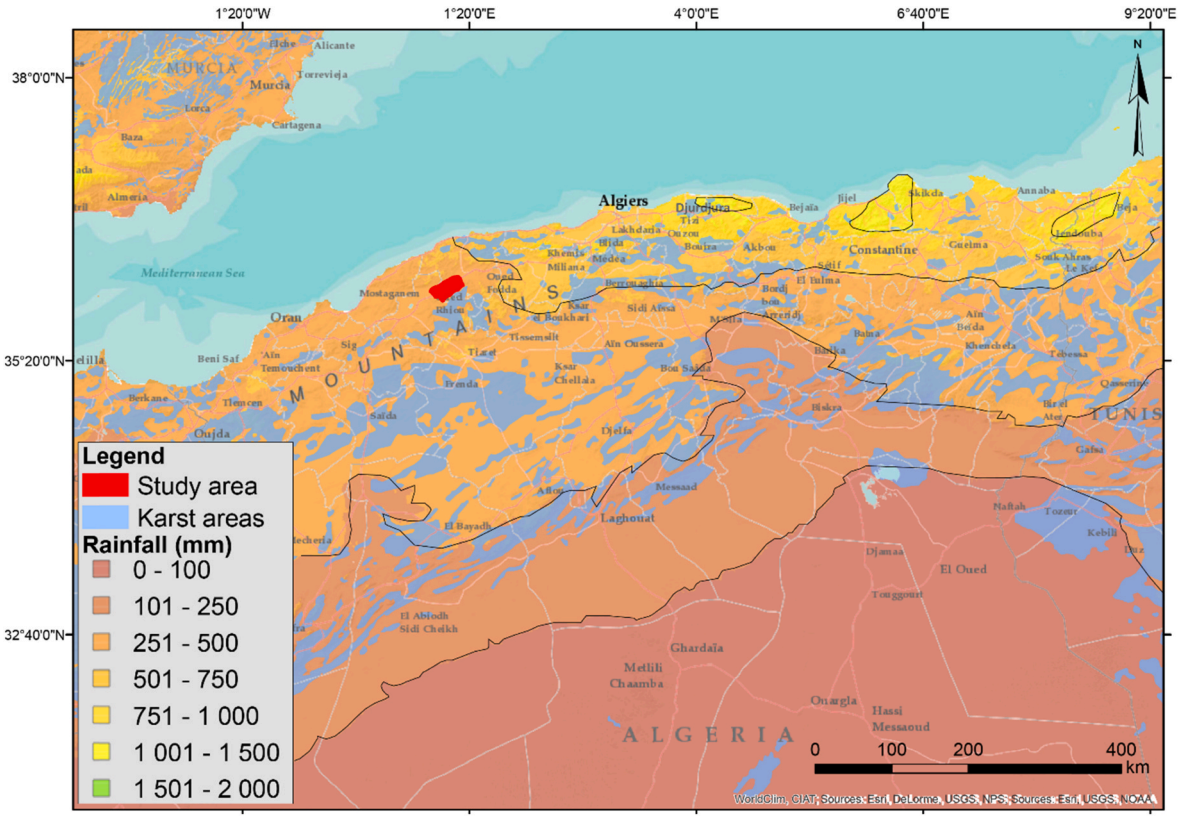


**Fig. 1.** Location of the study area in the karstic regions of Algeria. Repartition of rainfall in color. The karst areas comes from online arcgis data and the annual precipitation comes from WorldClim, CIAT.

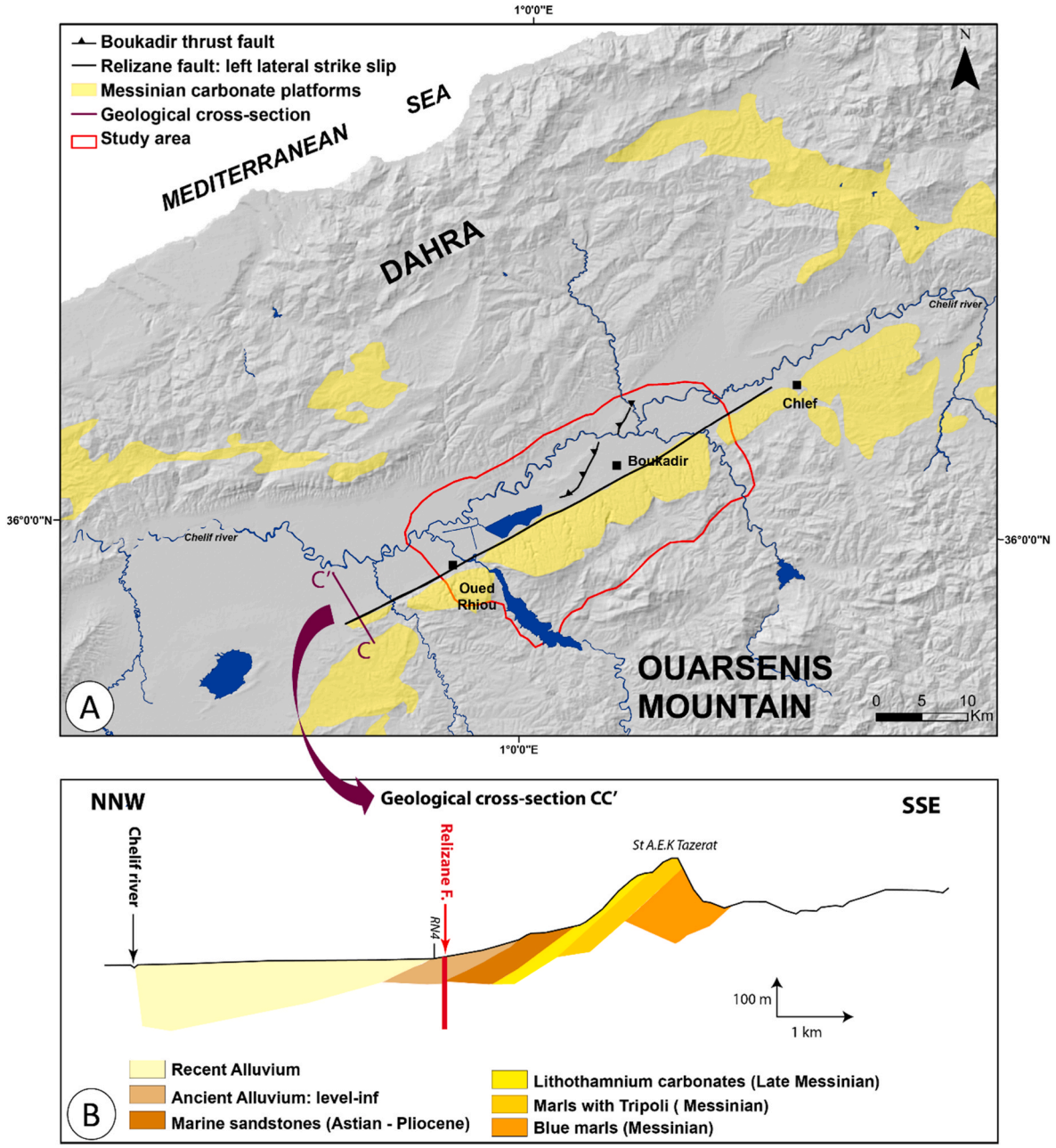


**Fig. 2.** A: Hillshade topographic map with locations of Ouarsenis Mountain range, Messinian carbonate platforms (in pink), main rivers (in blue) and local faults (black line) affecting the study area delimited by a red line. B: Geological cross section showing the geological organization of the study area.

*(Scet – Argi, 1985)*. The Chelif Basin in summer is called "tell furnace" or "portion of Sahara lost in the tell", because the heat is exceptional compared to neighboring regions *(Yacono, 1955*; *Boulaine, 1957)*. The Chelif valley is located south of the Dahra Mountains that form a barrier isolating the basin from the regulatory influence of the Mediterranean Sea (Fig. 2). The average temperature in Boukadir is 19.8 °C *(Bettahar, 2012)*, during the year, the temperature generally varies from 6 °C to 39 °C and is rarely below 3 °C or above 43 °C. Rainfall averages 361.5 mm/yr *(Bettahar, 2012)*.

## 3. Material and methods

We used different approaches and methods to understand and characterize karstic features in the Messinian Ouarsenis piedmont.

First, we used the geological analysis previously published in Moulana et al. (2021) to better understand the influence of lithological characteristics on the karst landforms and we present complementary data based on thin sections, geological field work and geological sections made at the level of the Boukadir quarry (Fig. 5). We analysed 7 thin sections taken in the indurated surface carbonate at the top of the Boukadir Quarry compare them to 12 thin section sampling carbonate at depth inside quarries. Dissolution features were also investigated in three quarries exploiting the carbonates (Oued Sly quarry in the east, Boukadir quarry and Sidi Abed quarry in the west (see locations in Fig. 3-A, appendix).

Second, we exploited unpublished drill hole data, section and electric profiles carried out by the general company of Geophysics (C.G.G) in 1966 existing in unpublished reports of the Algerian Ministry of Public Works. All data coordinates can be found in the appendix as well as the references to the reports. To investigate the site of the 1988 collapse sinkhole, we used the 150 m deep S1 drill core located 500 m to the south (Fig. 4). To document the carbonate platform geometry and the

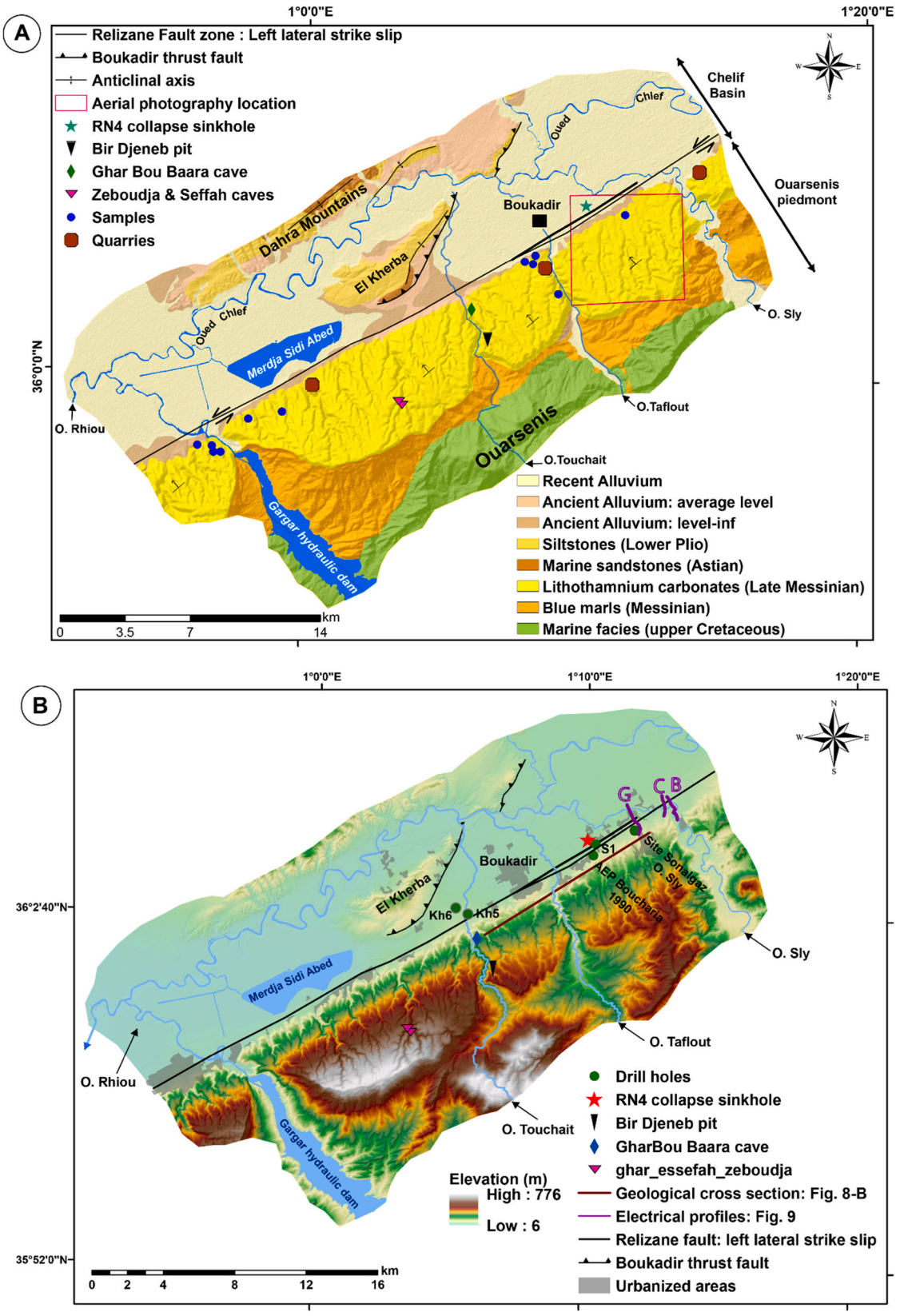


**Fig. 3.** Geological and hypsometric maps of the study area with key data used. A: Geology modified from geological map N°105 CHARON at 1/50 000 (Brives and Ferrand, 1912), with the location of thin section samples (blue dots), quarries studied (brown polygons), caves and the location of the aerial photograph used. B: Hypsometric map with the location of two major sinkholes (1988 RN4 and Bir Djeneb), electrical profiles location (purple line), main rivers, main drillholes used in this research (green dots) and caves. Spatial reference:WGS_1984_UTM_Zone_31N (Please add the spatial reference of the map).

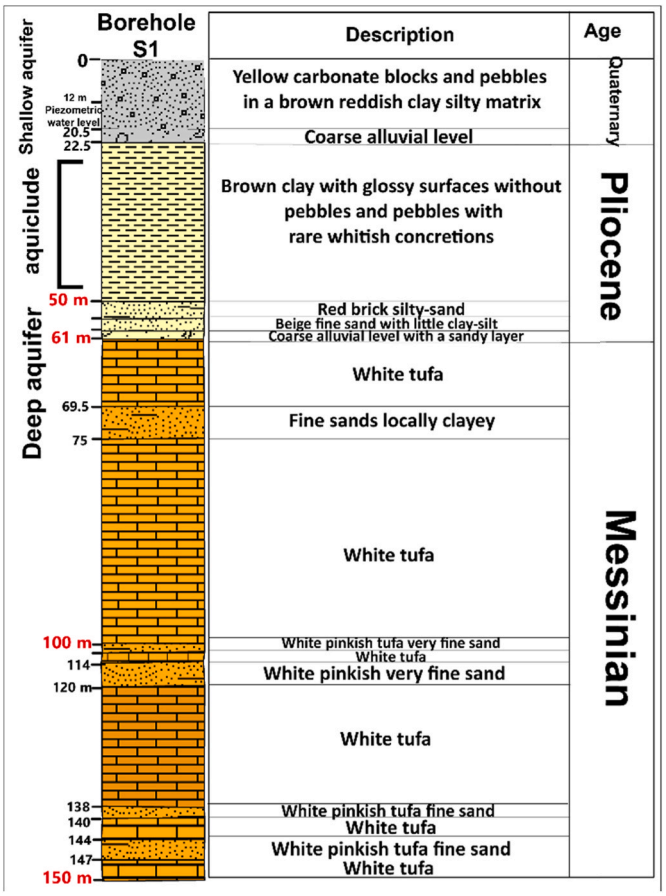


**Fig. 4.** Stratigraphic log of drillhole S1 located approximately 500 m south of the RN 4 collapse hole of 1988 (Fig. 3 - B) and carried out by the Central Laboratory for Public Works (LCTP) on 20/05/1989. This log shows Messinian carbonates at the depth of ~60 m (deep aquifer) below 26.2 m thick Pliocene brown clay formation (aquiclude) and 22.5 m thick Quaternary clayey-silty-sandy-conglomerate formations (surface aquifer).

stratigraphy at depth below the Plio-Quaternary cover, we used west of Boukadir, drill holes kh5 and kh6, and between Boukadir and Oued Sly, electric profiles (see location in Fig. 3-B). We displayed in Fig. 9 a representative electric profile, as all others show similar geometry except two electric profiles in Oued Sly River showing a different lithology. To provide information about the karstic dissolution of the Messinian carbonates at depth near the quarry locations, we revised a NW-SW section based on six ~100 m drill holes, used additional drill holes (AEP Bouachria, 111 m long, Site Sonalgaz O. Sly, 150 m long).

Third, to verify the influence of the fracture network in the genesis of karst landscapes in the field, we mapped the fracture network (Fig. 12-A, C, D and E) and completed it using the satellite imagery (Google Earth Images) (Fig. 10) and aerial photographs. Aerial photographs cover a restricted area located north of the piedmont between the cities of Boukadir and Oued Sly (Fig. 3-A and 15).

Fourth, our speleological analysis combined Birebent's work (1947 a and b; 1948) as well as additional field work.

Fifth, our geomorphological analysis was based on the observations of the different forms of dissolution on the ground, as well as on the cartography of the different karstic forms identified on satellite imagery (Google Earth images) and aerial photographs.

Finally, the climate analysis aimed to identify the triggering of the 1988 collapse and was based on two datasets. The first one is precipitation and evapotranspiration data from the "Climate Research Unit" (CRU; Harris et al., 2020). The CRU dataset (version 4) provides gridded monthly precipitation and evapotranspiration from 1901 to present with a spatial resolution of 0.5°. The CRU collects and interpolates weather observations and aims to obtain continuous spatio-temporal weather variables. Its main disadvantage is its coarse spatial resolution. The second exploited data is precipitation observations from four weather stations of ANRH: Oued Sly, Merdja, Ouarizane and Sidi Lakhdar (Fig. 6). Firstly, we analysed the change in precipitation using the CRU data as they are continuous over the period 1901–2019 and provide an overview of the rainfall conditions in this region. We also computed the aridity index as defined by Salem (*FAO, 1989*). This index is defined as PPP/ETP where PPP is the precipitation and ETP the potential evapotranspiration, calculated based on the method of *Penman (1948)* which takes into account atmospheric humidity, solar radiation, and wind. Secondly, we analysed the meteorological data coming from the weather stations to determine if they are consistent with the CRU data. Data are

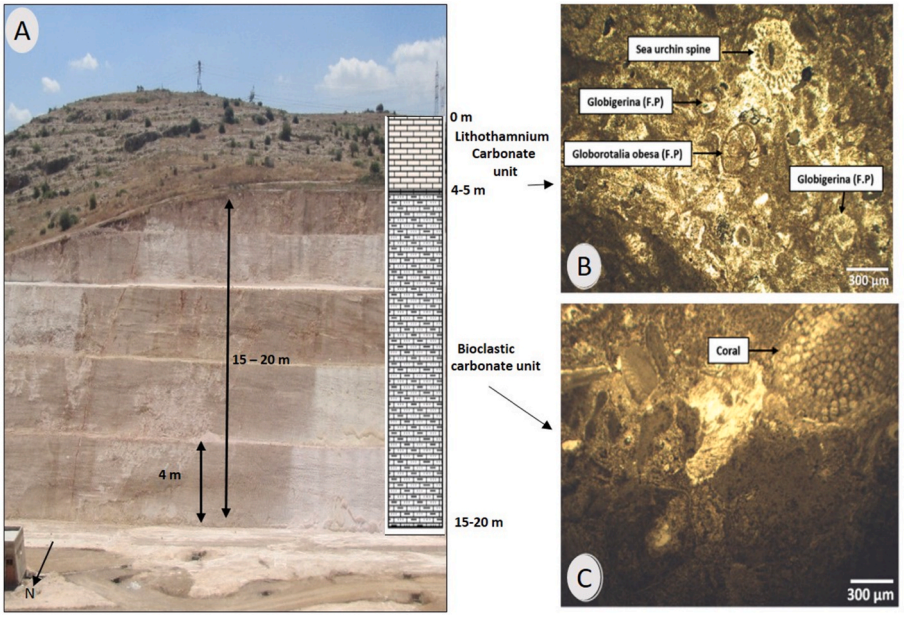


**Fig. 5.** Two types of carbonates evidenced: indurated compact one at the top (calcrete) and porous one (tufa) visible in the south side of the Boukadir quarry (A) and in thin sections (B & C). B- thin section in the calcrete. C- thin section in friable carbonate (tufa).

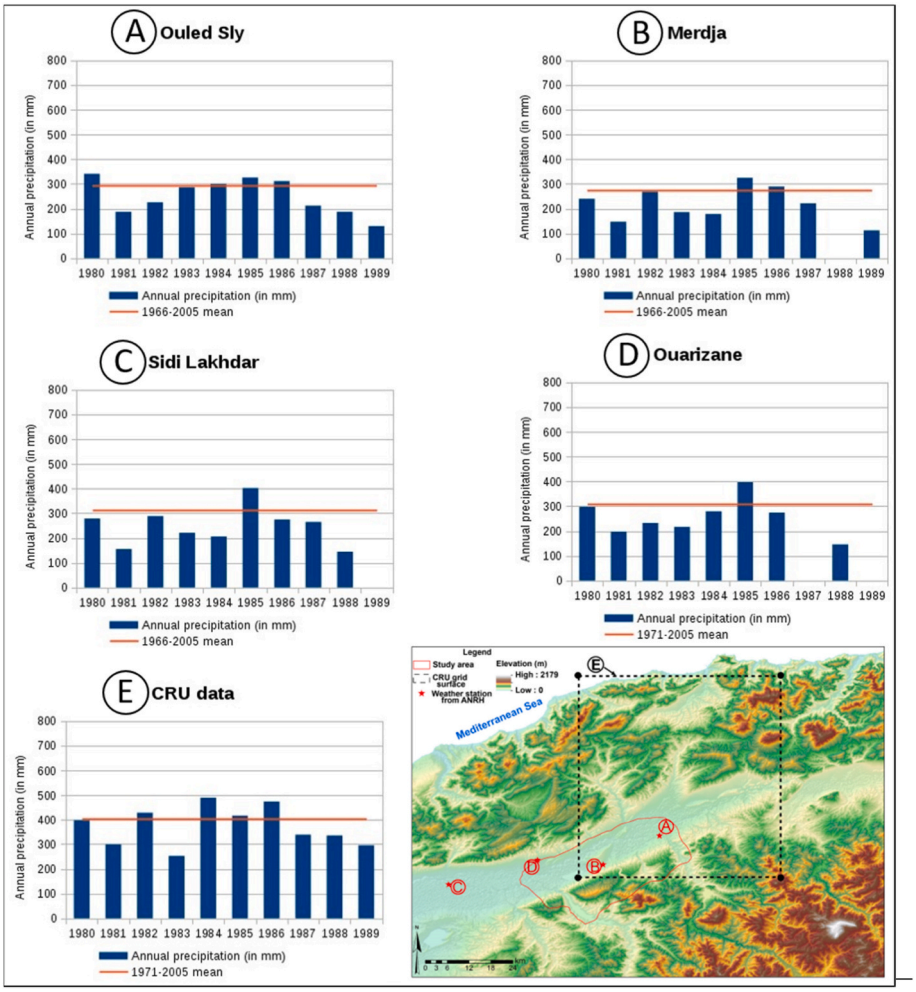


**Fig. 6.** Annual precipitation (in mm/year) observed (in blue) and the precipitation mean of the considered period (in red) in four weather stations (A to D) of the ANRH and provided by CRU (E). Bottom right inset: station locations and the selected CRU grid domain.

available on the period 1966–2005 for Oued Sly, Sidi Lakhdar et Merdja and 1971–2005 for Ouarizane. In addition, data include errors or lack of recording: 6% for Oued Sly, 9.6% for Sidi Lakhdar, 22.3% for Merdja, and 4.8% for Ouarizane. For these two different datasets, we analysed the annual precipitation amounts and their evolution focusing on the year 1988. We tried to answer the question: What was the rainfall pattern years prior to 1988?

## 4. Results

### *4.1. Geological characteristics of the carbonate platform and its deformation*

In the study area, the Messinian carbonates were deposited before the Messinian Salinity Crisis (Moulana et al., 2021). They consist in bedded bioclastic carbonates, with a sharp contrast between the two units. The upper Lithothamnium unit outcrops at the top of the platform and is composed of very homogeneous red algae carbonate beds with a variable thickness. Along the piedmont, this formation shows a thickness of at least 80 m *(Moulana* et al., *2021)* and a consistent nearly homoclinal ~ 5° dip. The lower bioclastic carbonate unit below is heterogeneous: bed thickness and facies display frequent lateral and vertical changes. This unit is also sometimes marly, with variable levels of cementation and characterized by burrows and serpulas of centimetric size. In the landscape, these two carbonate formations form staircases with marked discontinuities at bedding surfaces *(Neurdin-Trescartes, 1992*; Moulana et al., 2021*)*. Electrical profiles and boreholes show that the platform extends north under the Plio-Quaternary cover over ~5 km (Fig. 9).

Fieldwork in quarries along the Boukadir piedmont showed that the carbonates are friable in the mass (tufa) and covered by a layer of indurated carbonates (Fig. 4–A). Microscopic thin sections analysis revealed that the tufa is a packstone unit deposited in a high energy environment, composed of more than 95% of calcite with few traces of quartz *(Moulana* et al., *2021)*. These carbonates are characterized by a microsparitic matrix, a very well preserved primary sedimentation, and a large primary porosity. In the top indurated carbonates, thin sections show a well-developed cement, sometimes recrystallized, that is absent in the friable carbonates at depth *(Moulana* et al., *2021)* (Fig. 5–B). At the quarry top, the indurated carbonates are ~4 m thick (Fig. 5–A and B). These indurated carbonates are systematically present at the surface of the carbonate range, but this layer is much thinner (decimetric) along the valley walls.

The carbonate platform was uplifted and deformed by the left-lateral Relizane strike-slip Fault that follows the southern edge of the Chelif Basin. This transpressive fault strikes N70°E, a direction identical to the strike of the Chelif Basin. It runs over 150 km from the city of Chelif to the city of Relizane *(Meghraoui* et al., *1986*; *Derder* et al., *2011)*. However, its small-scale morphological expression in the Chelif Basin was not evidenced in remote-sensing data or in the field, suggesting very low present-day activity. The carbonate platform deformation still shows the following characteristics. First, deformation is changing along the fault

strike. Borehole data show that the depth of the carbonate platform below the Chelif Basin is changing at the location of the kh5 and kh6 boreholes the top of the carbonate platform lies at the depth of 126 m for kh5 and 175 m for kh6, which is different from what happens at S1 location (61 m). Second, the carbonate platform shows a changing tilt along the fault strike. The platform reaches the maximum elevation of 675 m to the west and 395 m to the east (Fig. 3-B) whereas the carbonate deposits show little change in thickness and facies. The platform was originally deposited at similar water depth *(Moulana et al., 2021)*. The change in relief is thus interpreted as a post-Messinian tilt and uplift of the platform in relation with the Relizane Fault activity. The main increase in relief occurs just after the intersection between the Relizane Fault and the Boukadir thrust fault and is interpreted as differential uplift at the fault junction. In addition, the outcropping carbonate platform is highly fractured (Fig. 10). Our satellite mapping evidences that the main fracture network has a NE-SW strike, subparallel to the orientation of the Chelif Basin. Fractures affecting the platform at the location of its highest elevation show significant vertical offsets (Fig. 10-B2). Few fractures have a south-north strike. Field work revealed a larger diversity of fault strike and dip than that evidenced by satellite imagery. The highlighting of these fractures in remote sensing data is linked to the fact that these subverticales fractures have an increased dissolution.

### 4.2. Characteristics of the karstic dissolution: the prevalence of solution pipes and deep karstification

Quarries were investigated to characterize macroscopic karstic dissolution. The following observations were made along quarry walls extending over more than 100 m. At the centric scale, the weathering is widespread, and there are frequent centimetric concretions of calcite resulting from its dissolution and recrystallization (Fig. 7-A) as well as centimetric pockets of dissolution (Fig. 7-B). In Oued Sly and Boukadir quarries, pluricentimetric horizontal cavities were quite frequently observed in tufa (Fig. 8-C). They are mostly independent of faulting. Finally, a single trace of a plurimetric cave, with stalagmites, stalactites and columns was observed in Oued Sly quarry (Fig. 7-C).

At the top quarries, there are vertical swallow holes (Fig. 11-A) dug in hard and compact carbonate. They are centimetric in size, with an elliptic to round shape and were found every 30–40 m. We thus infer that such small swallow holes must be frequent on the relief top. We interpret them as solution pipes. We evidenced one of these pipes in cross-section in the Sidi Abed quarry. It was located above a sinkhole, about 10 m in diameter and about 7 m deep (Fig. 11-B). Its top was in indurated carbonates, and below in the porous carbonate, the dissolved underlying conduit was filled with clay. In the valley walls of Oued Taflout, solution pipes filled with clays were also present (Fig. 12-B). No clear relation with faulting was evidenced. Small solution pipes related to faulting were evidenced only in relation with subvertical faults. These faults correspond to the ones mapped with the satellite imagery (Fig. 10). Inclined fractures were usually closed without macroscopic dissolution (Fig. 12-A, D and E). The origin of clay infilling solution pipes needs to be addressed. The Lithothamium carbonates are made of 95–98% of calcite *(Moulana et al., 2021)*, so the clay is infilling ihe pipes does not result from carbonate dissolution. The top of the quarries and most of carbonate platform are covered by a bare calcrete without any significant present-day soil. We thus inferred that the clay comes from an former, presently eroded, soil. Such a soil still exists and is visible on GE satellite images at the southern end of the carbonate platform, but it was not easely accessible and could not be investigated in the field.

In contrast to the low karstification inside quarries in the top 10 m, two boreholes near the piedmont close to the quarries evidenced that the ~150m thick carbonates are more strongly weathered at depth (Fig. 8-A). At the depths of 24 and 19m below a top carbonate tufa layer, a first karstic dissolution level is evidenced by a 15–30 m thick brown to red clay layer with calcareous gravels. At the depths of 54 and 59 m, a second karstic dissolution level is revealed by the absence of recovery in the drill holes. Similarly, in the cross-section based on 6 mechanical drill cores (Fig. 8-B), two wells between Oued Taflout and Oued Sly encounter the same first layer of karstic dissolution filled by 23–25 m thick red clay with carbonate gravels (reinterpreted from *Scet – Argi, 1985*).

An additional characteristic of the carbonates in the piedmont is their deep incision along the Taflout and Oued Sly rivers. The incision was plugged by later Plio-Quaternary deposits concealing it. It is evidenced in boreholes and electric profiles. The cross section based on drill holes in Fig. 8-B shows a 70 m deep incision in the carbonate at the location of the present Oued Taflout. The incision is filled with a basal

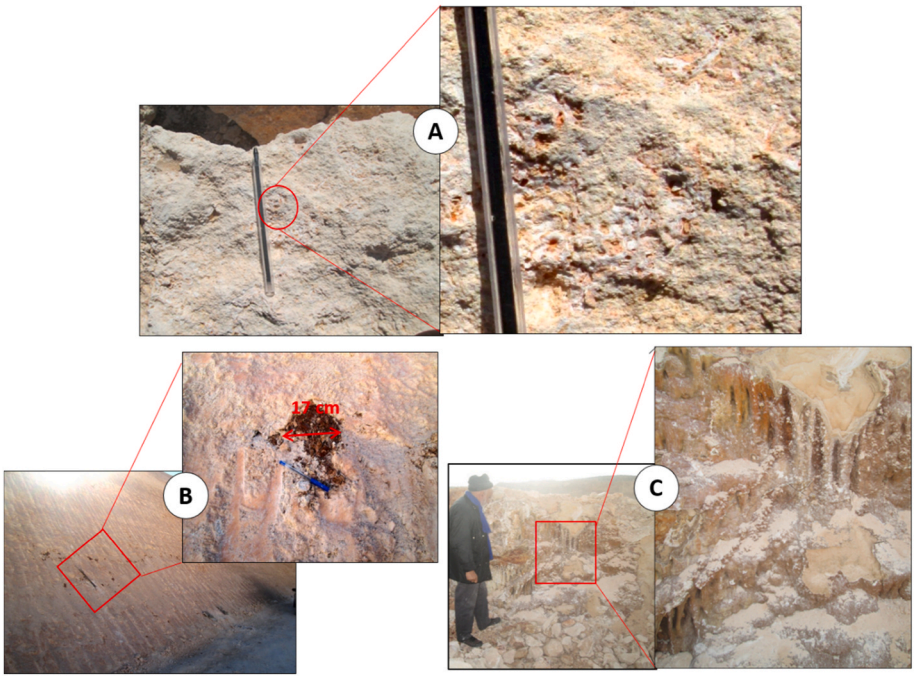


**Fig. 7.** Dissolution features within the carbonate massif at different scales visible in quarries. A. Typical centimetric scale dissolution and recrystallization in the tufas showing that the carbonate is deeply weathered (sampled from the base of Boukadir quarry). B. Layer with centimetric horizontal pipes filled by red clays (up to 17 cm in diameter) probably indicating a former phreatic level at the foot of the southern slope of the Boukadir quarry. C. Remains of a meter-scale cavity showing stalagmites in Oued Sly quarry. Quarries are located in Fig. 3-A.

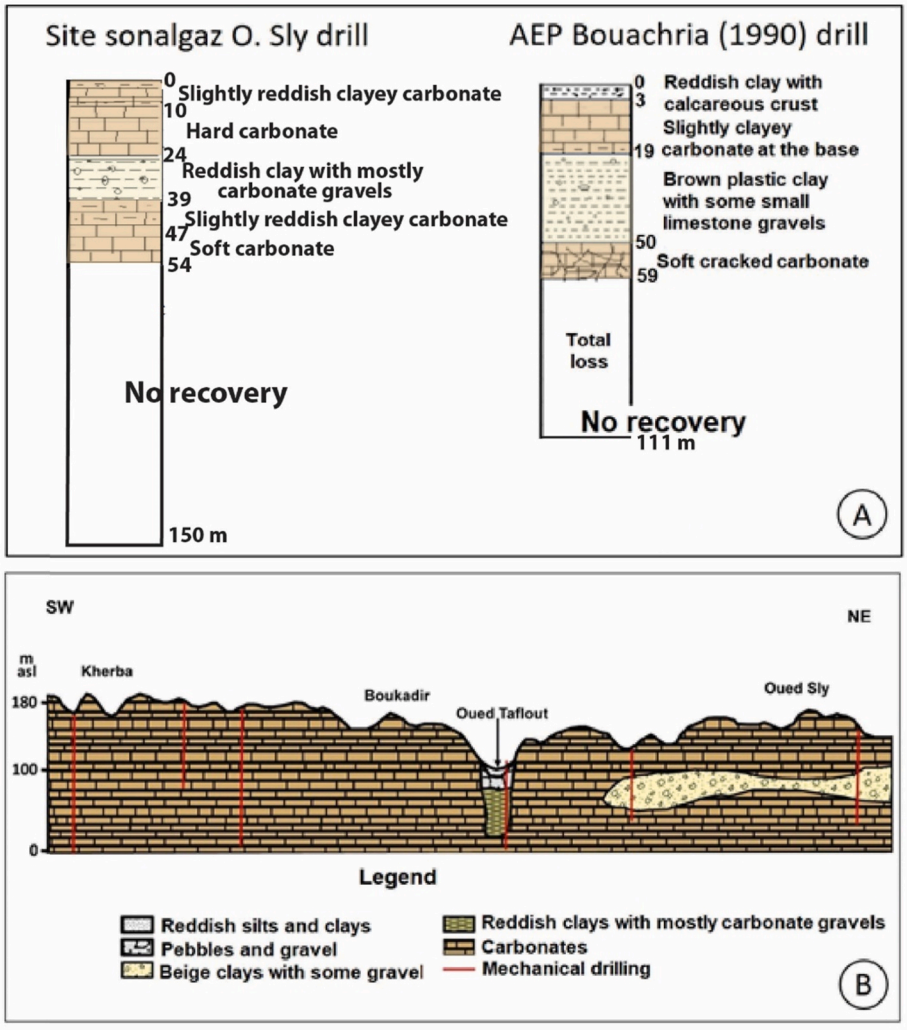


**Fig. 8.** A- Boreholes indicating the occurrence of a cavity filled by clay and carbonate pebbles (15 m high in the Site sonalgaz drill and 21 m high in AEP Bouachria drill). At greater depth, the fully weathered carbonates did not allow any recovery. B- Reinterpreted geological cross-section based on 6 mechanical drill cores parallel to the piedmont and across Oued Taflout (modified from Scet – Argi, 1985). Drilled holes also evidenced the occurrence of large cavities filled with clays and pebbles. Cross section location is indicated Fig. 3-B. The section shows a ~70 m deep Messinian incision at the location of Oued Taflout filled first by ~40 m of clay and then by coarser alluvial deposits.

35 m thick light brown clay unit with some gravels, then by a 30 m thick alluvium composed of pebbles and clayed gravels. The electric profiles at the location of the Oued Sly evidence the local absence at depth of the carbonates that are systematically present in other electric profiles to the west along the piedmont (Fig. 9).

Large karstic dissolution features father north inside the carbonate Ouarsenis are rare, but five sets of caves were described by Birebent (1947a) (see coordinates in Appendix). The two large ones called Bir Djeneb and Ghar Bou Baara are located in the lower bioclastic unit. The others are located in the upper Lithothamnium carbonate unit. We describe their characteristics in the following.

The most considerable karstic feature, the Bir Djeneb or « le puit du Diable», is located 5.5 km SW of Boukadir (Fig. 3). The opening is a wide circular depression in the eastern flank of Oued Touchaït forming a cylindrical pit with vertical walls about 20 m in diameter and 63 m deep (Fig. 13-right). The morphology of the Bir Djeneb is thus similar to the RN4 pit. The former is dug mostly in unconsolidated sediments. At the top, the pit walls are colluvium deposits made of pebbles with little or no matrix. Below, they are more clay-rich sediments. In the bottom, a narrow conduit about 3 m in diameter goes down in the carbonate with a low slope to reach 73 m deep. This narrow conduit is inclined by 45°. The bottom of the main shaft is made of scree, as well as the floor of the small conduit. The latter ends in a second cave, smaller than the main pit, 5 m deep and 3 m in diameter *(Birebent, 1947a)* (Fig. 14-C). The second large cave, Ghar Bou Baara, is located on the western side of the valley of Oued Touchaït (Fig. 3). It is ~2 m high and 76 m long subhorizontal cave (Fig. 14 A, A' & C). The main passage displays a rather constant width and a meandering course oriented N-NE. The slope is gentle, parallel to the dip of the carbonate formation. At the upper end, the passage is partly filled with sediments. The meandering morphology of this cave suggests an ancient underground river. The entrance of the cave is probably an ancient resurgence *(Birebent, 1947a)*. Other caves are smaller, horizontal and narrow. Fig. 14-C' displays the cave morphology of Ghar Seffah and Ghar Zeboudja caves closely located (Birebent, 1947 a). The Ghar Seffah cave is a subhorizontal cave about 15 m long. The low slope of the gallery indicates that this conduit was formed by water seepage from the ceiling. The Ghar Zeboudja cave is about 13 m long and results from carbonate dissolution along a large joint separating strata. Both conduits drain the Boukadir Massif.

### 4.3. The 1988 collapse pit

The 1988 collapse opened in the middle of National 4 highway between Oued Sly and Boukadir, 1.5 km north of the outcropping carbonate piedmont. It is 60 m in diameter and 35 m deep with vertical walls (Fig. 13-left). The corresponding volume is about 95 000 cubic meters. This volume implies the presence of a huge underground void before the collapse. Concentric cracks appeared all around the sinkhole over a radius of about 250 m, affecting the surrounding dwellings. The hole was rapidly filled with water (up to 12 m below the ground level). Measurements by the civil protection service and the scuba diving team show that the average water depth was 23 m. As the hole opens at an

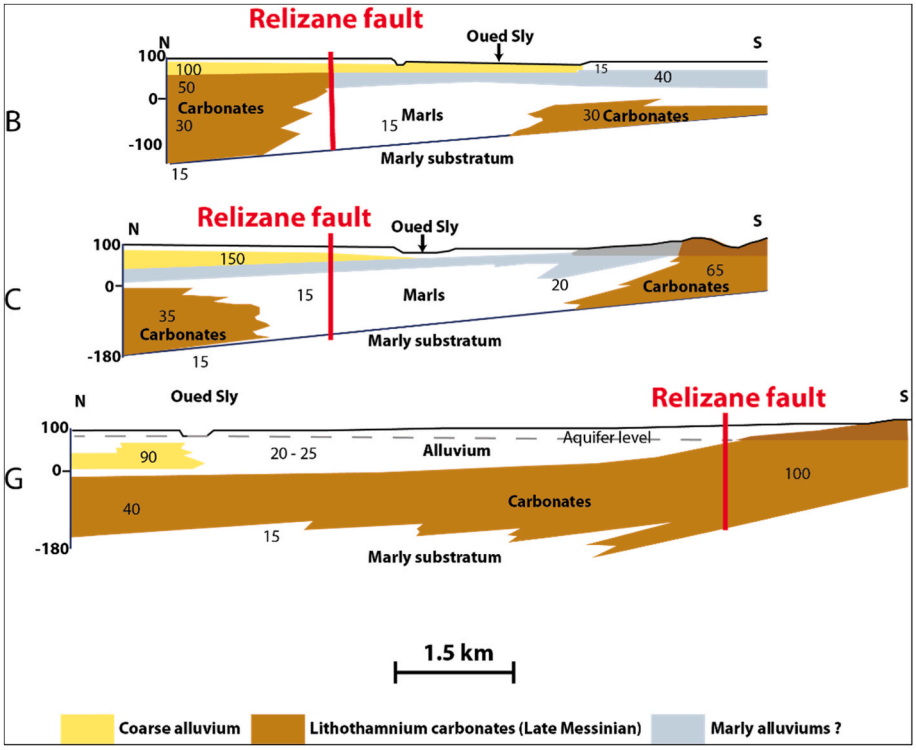


**Fig. 9.** Electrical profiles extending northward from the piedmont where carbonates outcrop (modified from C.G.G, 1966). Profile G is a typical profile, identical to others between Oued Sly and Oued Tafl-out. Profiles B and C show a deep erosion of the carbonates at the location of the Sly Valley filled by marly sediments. This incision is interpreted to be related to the Messinian salinity crisis. Value number indicate resistivity. Electrical profiles location is indicated Fig. 2-B. (modified from C.G.G, 1966).

altitude of about 90 m asl and is 35 m deep, the floor of the void must be much lower than 55 m above sea level (asl).

The stratigraphy at the location of the collapse was investigated thanks to the nearby borehole S1 (Fig. 4) to identify the location of the initial void. The top unit is a 22.5 m thick alluvial formation. It is composed of clayey, silty and sandy conglomerates, and corresponds to the Plio-Quaternary surface aquifer systematically present in the western Middle Chelif Basin (Perrodon, 1957; *Mattauer, 1958*; *Bettahar* et al., *2008*). The underlying 26.2 m thick unit 2 composed of brown clay is interpreted to be a lacustrine deposit and an aquiclude. Below this layer, the 11 m thick continental unit 3 is composed of a basal coarse alluvial level overlain by a sandy layer. Then from the depth of 61 m to at least 150 m, unit 4 shows chalky white tufas. It corresponds to the carbonate platform outcropping to the south, and forms an aquifer that have a different hydrogeological potential compared to the upper one (*Bettahar* et al., *2008*). The carbonates are friable and contain ~90% or more of CaCO3. They are thus similar to the Messinian carbonate packstones we sampled in the quarries. Given the observed stratigraphy, we infer that the initial void responsible for the collapse was located in the carbonates.

### 4.4. Geomorphology

The Messinian carbonate platform looks like a slow dipping slab ending abruptly to the southeast with a nearly vertical scarp at the contact with the more erodible Blue Marl Formation forming a cuesta (Fig. 15). It is incised by a very well developed dendritic hydrographic network. It is thus similar to a dissected pediment.

The geomorphological analysis based on field work, aerial photography and imagery allows identifying different karstic phenomena: shelter caves, small sinkholes, swallow holes (ponors), and resurgences.

The most frequent surface karstic dissolution features are shelter caves (Fig. 14-B). Field work shows that they are mostly metric in size and can be found on every valley wall. Their interior is composed of pinkish white tufas, and their external roof consists in a thin layer of hard and indurated carbonates similar to the one at the quarry tops (Fig. 5-A). The floors and tops of most shelter caves are mainly located along bedding joints, which are preferential paths for the underground water flow because of their high permeability. Some of these are associated with a phreatic network as assumed in the Bou Baara cave (Fig. 14-A and A'). Satellite images shows that close to fractures, the shelter cave morphology turns into a ruiniform landscape due to enhanced dissolution. Their frequency seems to be independent of the relief, the valley size and the upstream drainage, but a function of lithology. In the lower bioclastic carbonate unit that has more permeable beds favouring dissolution, they are more frequent. Independently of lithology, satellite images show an additional specificity regarding their spatial distributions (Fig. 18). They are nearly systematically present close to present-day carbonate river beds not covered by sediments. Above river beds, some are aligned at similar elevation, and forms successive steps, a characteristic reminiscent of bedrock terraces.

On the aerial photography, we identify one ponor, distinguished when the secondary stream suddenly end. We also mapped four circulars depressions on the bare carbonates.

On the field, we observed very few large resurgences. According to Birebent (1947b), the main ones feed the Merdja (Fig. 15), which is a marshland 6 km long and up to 2 km wide in front of the carbonate piedmont, south of the Chelif river. Farther west, there is another much smaller resurgence, located in the weathered carbonate of the lower carbonate unit, near the road leading to Gargar hydraulic dam (Fig. 15).

### 4.5. Climatological analysis

The long-term precipitation evolution was analysed. Fig. 16-A shows the fluctuations in CRU precipitation around the 1960–1989 mean (435 mm), from 1901 to the end of the 1970s. From 1977 to the early 2000s, the 10-year running mean was below the 1960–1989 average indicating a period with a precipitation deficit. During this period, some years present precipitation values below the 1960–1989 mean minus one standard deviation (435–93 = 342 mm). These years indicate a significant precipitation deficit: 1977, 1981, 1983, 1987 and 1988 with respectively 327 mm, 299 mm, 252 mm, 338 mm, and 335 mm. After the

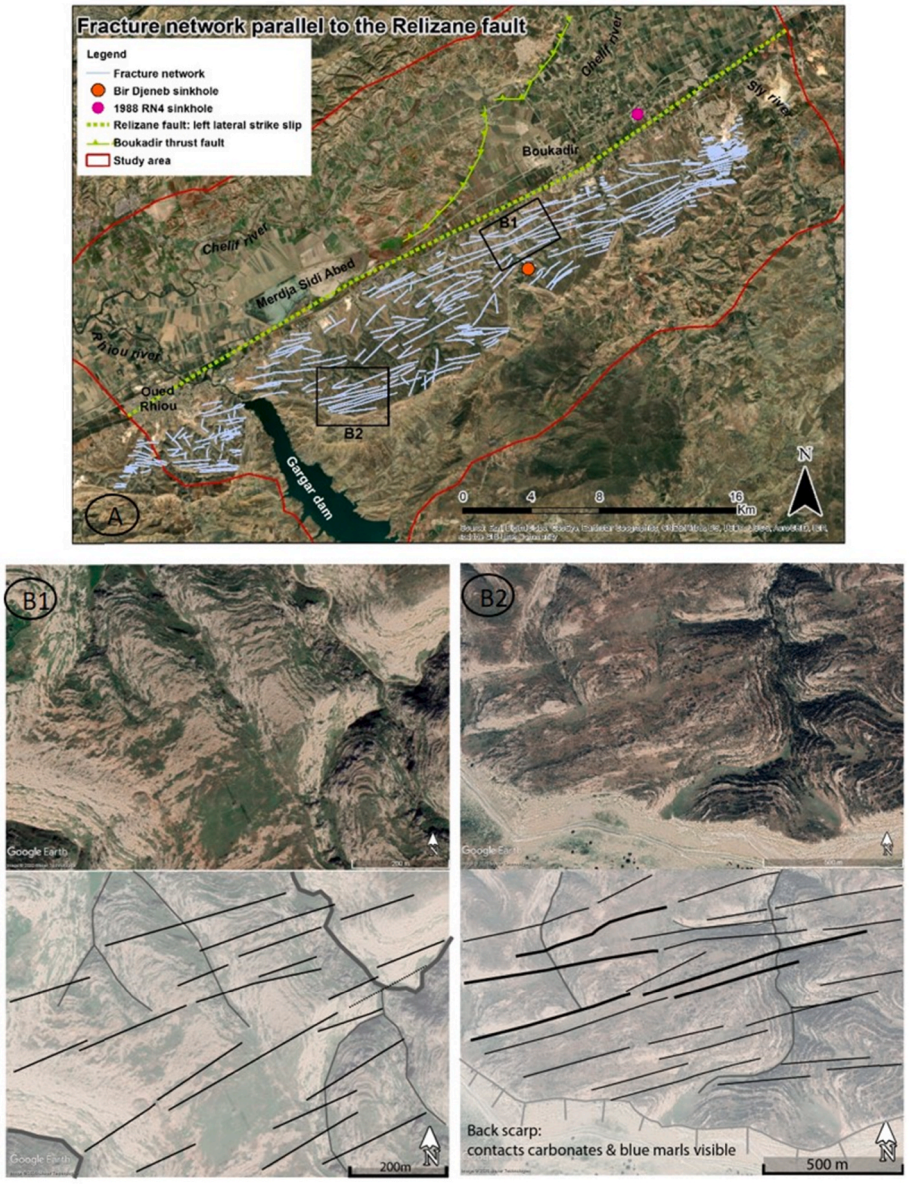


**Fig. 10.** A. Google Earth Image showing the fracture network parallel to the Relizane Fault. B. Details of the fracture network mapped using very high-resolution satellite images from Google Earth.

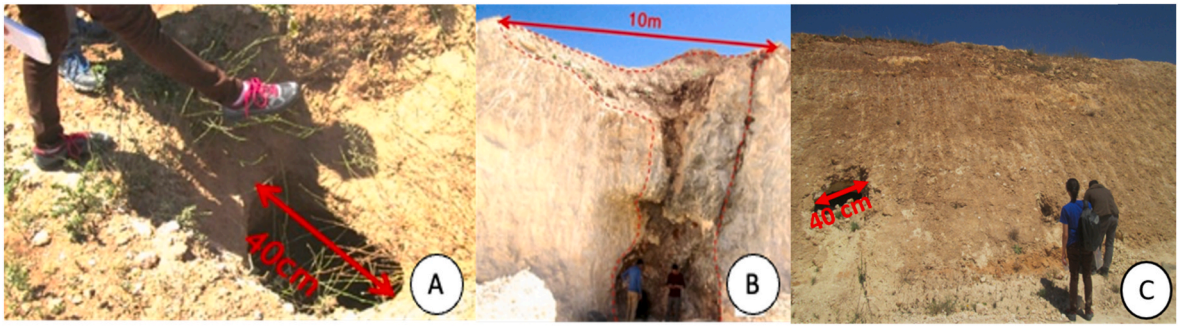


**Fig. 11.** Exokarst on the top of the carbonate massif at different scale. A. decimetric solution pipe (top of Boukadir quarry) quite frequent in the area. B. Remains of a solution pipe that became a sinkhole (Sidi Abed quarry). C. Decimetric horizontal solution pipes observed on the top of the Boukadir quarry.

early 2000s, precipitation appears to increase again, ending this precipitation deficit period.

Fig. 16-B shows the FAO aridity index calculated on CRU data (see Materials & Methods; Salem (1989)). The aridity index supports the results obtained with the precipitation only (Fig. 16-A). Indeed, this index oscillates around the 1960–1989 mean before the 1970s, then it

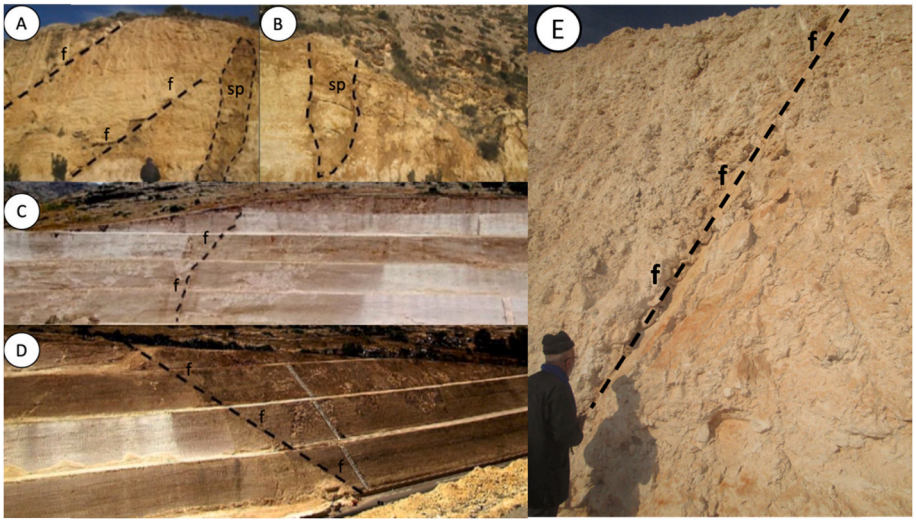


**Fig. 12.** Fractures (f) and solution pipes (sp) some independent of fractures. A and B. Solution pipes mainly filled with clay and oblique fractures without filling (Oued Taflout). C. Subvertical fault underlined by red clays (SE slope of the Boukadir quarry). D. SE-NW inclined fault without filling (SW slope of the Boukadir quarry). E. Inclined SW-NE fault without filling (SW side of the Oued Sly quarry).


**Fig. 13.** The 2 major sinkholes in the study area. Left. The 1988 RN4 sinkhole in the Chelif Basin, 500 m from the carbonate piedmont (Photo taken by Pr. Mostefa GUENDOUZ on 16/06/1988). Water table is 12 m below the level of the road. Right. The Bir Djeneb in the carbonate Ouarsenis Mts.

decreases during the 1970s and remains below the 1960–1989 mean until the early 2000s when it increases again. During the whole period (1901–2019), the aridity index remains constantly within the semi-arid range (*Salem, 1989*). However, this aridity index approaches the arid zone threshold of 0.2 during certain years including 1987 and 1988 with an index of 0.27, and more strongly in 1981 and 1983 which have an index of 0.24 and 0.20 respectively.

Finally, the year 1988 occurred at the beginning of the deficit precipitation period but 1988 was not the first driest year. During previous years, 1977, 1981, 1983 and 1987, there was also a high precipitation deficit according to the CRU precipitation data.

Using the weather station, precipitation evolution in the study area was confirmed. As mentioned in the Material and Method section, weather station observations are recorded over different time periods and contain missing data (Fig. 6 A to D). Therefore, the analysis cannot be complete and must be carried out with the usual precautions. As shown by Fig. 6, although the four weather stations did not record the same amount of precipitation every year, they show some similarities. First, the year 1988 corresponds to a low amount of precipitation over the considered period. Second, the year 1985 (and/or 1986) corresponds to a maximum of precipitation over the considered period. Third, between 1985 and 1988, precipitation decreased. Finally, the years 1987 and 1988 are below the mean precipitation over the considered periods. Fig. 6-E, which represents precipitation data from the CRU over the same period, corroborates the results.

## 5. Interpretation and discussion

### 5.1. Present-day karst

The geological and the geomorphological results show that the current surface weathering is weak (rare sinkholes and ponors) and the extent of the currently active karstification is limited, in accordance with the studies of Birebent (1947a,b, and 1948). Inside the massif, the dissolution is mainly active in the multiple sub-vertical fractures mapped (Fig. 12) and in the frequent small shallow solution pipes evidenced (Figs. 11 and 12-A) allowing rainwater to infiltrate. Solution pipes independent of the fracturing are one of the main component of the exokarst. For Lipar et al. (2015), solution pipes are vertical tubular karst voids formed in carbonate rocks with matrix porosity, reported and described worldwide. Willems et al. (2007, 2018) show that vertical solution pipes can indeed be related to punctual infiltration of water in terrains overlying hardened carbonates (calcarenites), without any subvertical fracturations. We found a similar situation in the karst of Boukadir.

This atypical karst area is also characterized by a well-developed surface hydrographic network (Fig. 15). It is an uncommon feature, because the carving of the dendritic stream network implies the

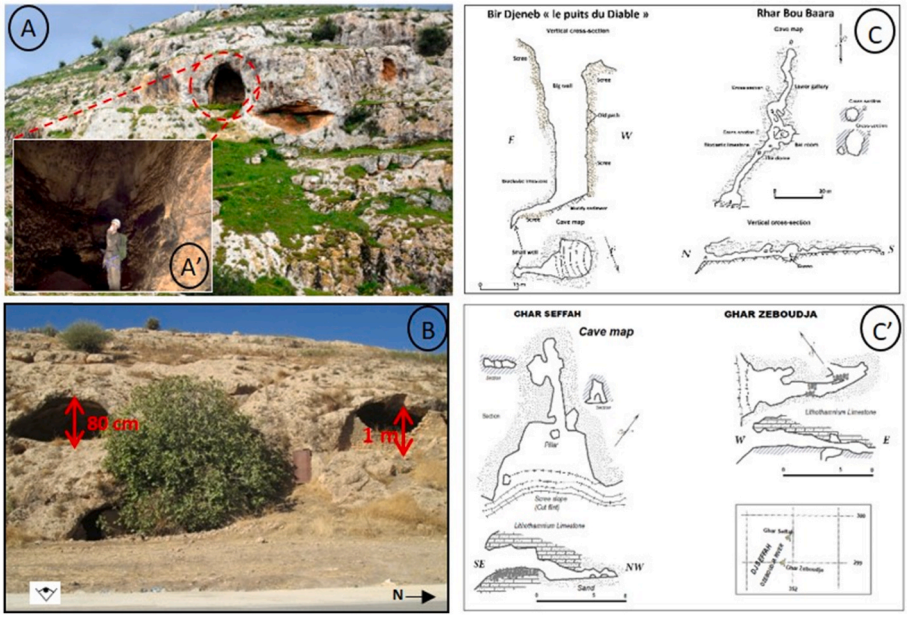


**Fig. 14.** A & A'. Ghar Bou Baara in the carbonate Ouarsenis Mts (photo taken by a caver Abdelaaziz SABER). B. Shelter caves (epikarstic semi-horizontal dissolution forms) between carbonate beds near the Taflout River, eastern part of the study area. C and C'. Maps and cross-sections of four caves (Bir Djeneb, Ghar Bou Baara, Ghar Seffah and Ghar Zeboudja) of the northern Ouarsenis piedmont modified from Birebent (1947a).

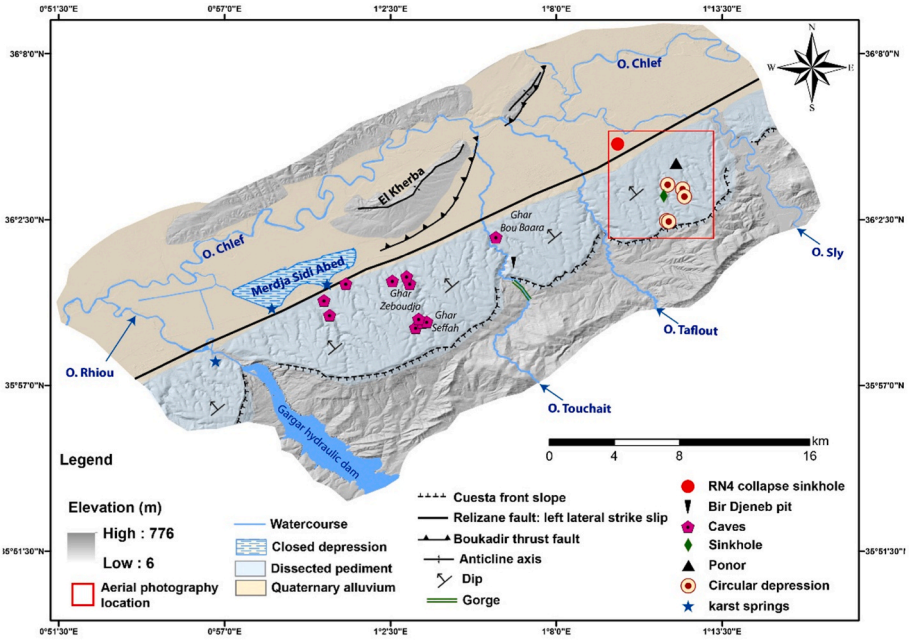


**Fig. 15.** Geomorphological sketch of the study area. Inside the red rectangle, a ponor, circular depressions and a sinkhole were mapped based on an aerial photography. Caves location come from Birebent (1947a a).

occurrence of significant recurrent surface runoffs and concentrated flows. The high drainage density observed may be related to the 4–5 m thick layer of indurated carbonates with a low porosity covering the top of the Ouarsenis carbonate massif (Fig. 5-A). The thick induration is interpreted to be similar to a calcrete. It would have progressively decreased the infiltration and would have led to a reduction in dissolution in the massif. Calcretes are the product of weathering predominantly in arid and semi-arid regions (*Goudie, 1983*; *Esteban and Klappa, 1983*. *Wright and Tucker, 1991)*. In the thin sections sampling the indurated carbonates, we observed a widespread micritic calcite matrix which is precipitated within the intergranular pores of the Lithothamnium carbonate packstones, and a mosaic of calcite crystals of different sizes (Fig. 5B and C). These characteristics are typical of calcretes (*Esteban and Klappa, 1983*; *Wright and Tucker, 1991)*. Their origin is related to the dissolution of $CaCO_3$ during rainfall and its later precipitation during intense evaporation in the dry season (*Gocke* et al., *2012)*. In addition, the Boukadir area is highly favourable to calcrete formation. Indeed, it is a semi-arid region with a strong seasonality: the dry season lasts from May to August, and a more humid period from September to April (≈53 mm). The calcrete thickness is greatest at the top of the carbonate outcrop, but calcrete is widely present on all carbonate surfaces and particularly at valley bottom not covered by

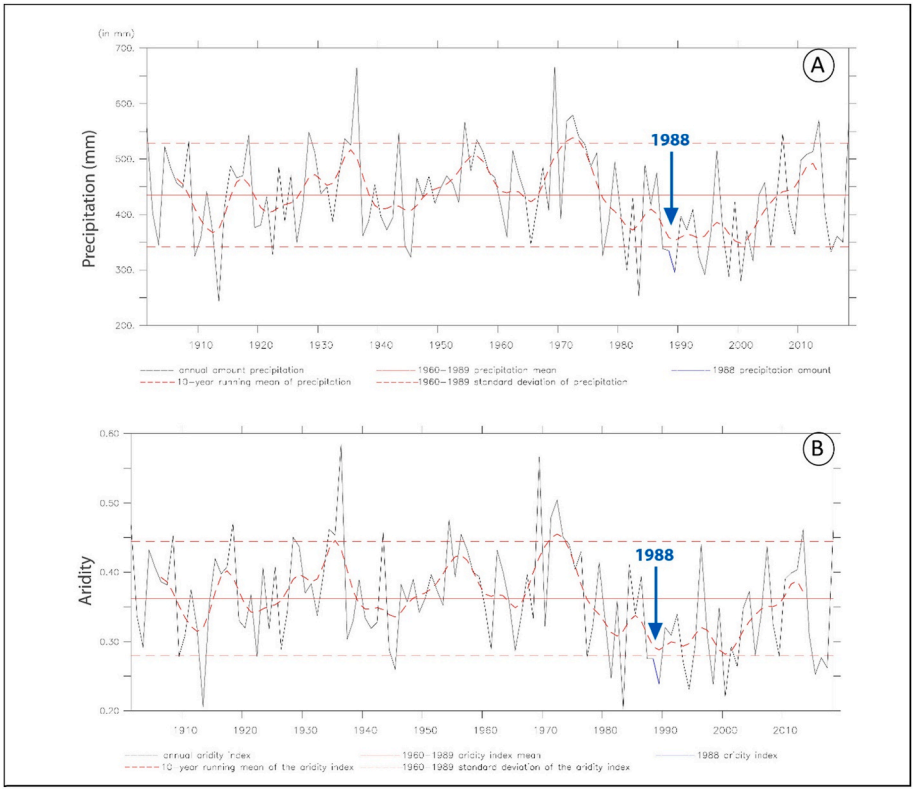


**Fig. 16.** Annual CRU amount of precipitation (top) and aridity index (bottom) from 1900 to 2019 extract from the nearest grid point of Boukadir (see extent on Fig. 6-E). A/B: amount of precipitation (in mm/year)/aridity index in solid black line, 10-year running mean of precipitation/aridity index in bold dashed red line, 1960–1989 mean precipitation/aridity index in solid straight red line, ± 1 standard deviation in dashed straight red lines and the 1988 precipitation amount/aridity index in solid blue line.

sediments.

In addition to the calcrete that reduced dissolution in the massif, several other factors explain the current low degree of karstification. First, the present semi-arid conditions in the study area do not favour an intensive dissolution. This semi-arid climate has frequently been predominant since the Pliocene *(Ballais and Cohen, 1981)*, but glacial periods were more humid. Second, the lack of a humic-rich soil and of an abundant vegetation implies a low biogenic $pCO_2$ that is necessary for an efficient dissolution of calcium carbonate bedrock. Third, the high porosity of the carbonate platform in the form of packstones *(Moulana et al., 2021)* visible in the quarries allows a high diffuse infiltration. Karst is generally less developed in poorly consolidated rocks where infiltration is diffuse than in compact limestones where infiltrated water is concentrated along fissures *(EK, 1976)*.

Another specificity of the studied karst is its shelter caves. They have a complex development. As their interior is easily hollowed out, human dug these sites to enlarge them to house sheeps, and, in some places, to extract phosphorite to improve the arable soil *(*Birebent, 1947 a*)*. Regarding their natural development, shelter caves in karst terrains are generally remnants of old caves reworked by surface processes or cave springs that were left high and dry by the downcutting of river valleys and the lowering of the water table (Shelter type 1 or 2 in Fig. 18). This is the case of the shelter caves associated with the Bou Baara, Ghar Seffah and Ghar Zeboudja caves (Fig. 14-A, C and C'). However, shelter genesis in Boukadir is not generally interpreted as resulting from the erosion of phreatic caves, because shelter frequency is much larger than the documented caves. We infer that most shelter caves are epikarstic, through some may be related to former phreatic levels. We interpret them as a product of differential weathering in relation with calcrete cementation or with change in carbonate lithology, because they develop in crumbly weathered carbonates with a roof in more cemented and cohesive carbonates (Shelter type 3 in Fig. 18). Regarding the later case, fracturing and initial difference in carbonate facies lead to the occurrence of more porous and soft carbonates and of more consolidated ones. For example, the upper carbonates at the top of the Ouarsenis Massif are, in general, more resistant and homogeneous than the lower bioclastic carbonates. The upper carbonates are dominantly composed of Lithothamnium, an encrusting red-algae with numerous thin films that play an important role in the early internal cementation of reefs and algal crusts in the marine environment *(Alexandersson, 1974)*. We infer that the difference in carbonate facies influence the geometry, occurrence and morphology of the shelter caves, because they are more frequent and have different sizes according to carbonate lithology. However, independently of the initial erodibility of the carbonate facies, we consider that the most important factor regarding the origin of shelter caves is calcrete outcropping on all carbonate surfaces in the Ouarsenis Piedmont. Indeed, rooftops at the shelter entrance are made systematically of more indurated carbonates, i.e. calcrete, than inside made of porous carbonates, i.e. tufa (Fig. 18). As a consequence, the shelter size depends on the thickness of the calcrete and the strength of the carbonate tufa. Calcrete cementation is a current process in its river valleys because calcium carbonate is preferentially dissolved at the mountain top and is then precipitated in the bedrock river below given the current climate *(Ek* et al., *1981*; *Mathieu* et al., *1983)*. The present-day bedrock riverbanks in the southern part of the carbonate piedmont are the place where the relationship between shelter caves and calcrete is best evidenced. There, shelters are often located along riverbanks and as well as above the river beds at different elevation in valley flanks (Fig. 18). This stepped shelters landscape is interpreted to result of the incision and the lateral erosion of rivers. To summarize the different possible origins of shelter caves, a schematic representation of their different type are presented in Fig. 18 (top).

In Boukadir, the Quaternary karstification is thus mostly characterized by the precipitation of carbonates, isovolumetric weathering and solution piping independent or along fractures. Active dissolution features forming large phreatic caves are not predominant during this period.

### 5.2. Origin of the deep karstification in the uplifted ouarsenis carbonates

In the carbonate piedmont, we documented the occurrence of rare caves. The first one, Bir Djeneb (Birebent, 1947a,b, *1948*). We questioned the following assumption: the hole is far from the talweg of the Oued Touchaït and considering how similar this shaft is to the 1988 pit of the RN4, we infered that Bir Djeneb is a collapse pit open by the breakdown of the roof of a deep cave in the bioclastic carbonates. This deep cave as well as the other phreatic caves in the Ouarsenis carbonate piedmont like the Bou Baara cave (Fig. 14-A and A') are interpreted in relation with the progressive uplift of the platform during the Plio-Quaternary induced by the transpressive motion (*Meghraoui, 1988*). The uplift triggered a progressive drop in the local river base level, and successive abandonment of former phreatic levels in the massif, a mechanism that also explain the occurrence of shelter caves at different levels along river valleys (Fig. 18-top). This is a classical example in karstology.

### 5.3. Origin of the 1988 collapse shaft and adjacent deep karstic dissolutions: the base level drop during the Messinian Salinity Crisis

As shown on Fig. 13-A, the 35 m deep 1988 collapse occurred through a thick pile of sediments that comprise 22.50 m thick Quaternary alluvium and 27 m thick Pliocene clay deposits. The collapse was associated with circular fissures up to 250 m from the center of the shaft. Even if the upper terrain is composed of unconsolidated and relatively insoluble material, we infer that the collapse is due to breaking down of an underlying cave roof. This process is thus karstic. Messinian carbonates, that outcrop 1.5 km to the south, lie at 61 m depth and a huge void should have existed in this formation to let the place for a collapse volume of at least 95 000 cubic meters. Such a phenomenon is similar to features observed for example in Belgium. In this country, collapses have occurred since 1910 in the Scheldt valley which is filled by 50 m of sedimentary cover (*Derijcke, 1979;* Delattre, 1985), and some show circular fissures extending to about 250 m of the collapse center like in our case study. These collapses were related to heavy industrial pumping which lowered the aquifer level in caves formed in Carboniferous limestone 50 m below the surface. The lowering of the carbonate aquifer caused the replacement of water by air whose lower density did not support the weight of the cave roofs, causing their collapse. The falling of the cave ceiling spread to the upper formations. Like in Belgium, a lowering of the acquifers in the Boukadir region may be one factor of the 1988 collapse. Our climatic analysis showed that very dry years occurred in 1977, 1981, 1983 and 1987 leading to a high precipitation deficit before 1988 (Figs. 6 and 16). In addition, this period of precipitation deficit extended over the whole Maghreb (Sebbar et al. (2011) in Morocco, Kingumbi et al. (2009) in Central Tunisia, and Meddi et al. (2014) in northern Algeria). The Chelif plain recorded the highest precipitation deficit, i.e., 56% (Meddi et al., 2014). As mentioned by Kingumbi et al. (2009), this deficit was probably influenced by the ENSO oscillation. The collapse sinkhole in 1988 was thus probably associated with a progressive drop in the upper alluvial and deeper karstic aquifers. Tighilt (1990) measured a drop in the alluvial aquifer from 8 m in October 1983 to 12 m in March 1989 near the collapse. However, the connectivity between the aquifers is uncertain. The case is not classical because of the unclear role of the Relizane fault and associated deformation. So, an in-depth understanding of the 1988 collapse requires a modelling of the functioning of the upper and deep aquifers and of the Relizane Fault.

Imprints of two deep karstification levels in the Boukadir piedmont 1.5 km south of the 1988 collapse were also evidenced (Figs. 8 and 9), the upper level is filled by red clays with few carbonate pebbles, the lower one is at least 55 m below the surface and open. The deepest voids are at an elevation similar to the deep incision in the carbonates at the level of the Taflout and Oued Sly Rivers (Figs. 8 and 9). They are at higher elevation than the deep cavity related to the 1988 collapse, but it could be related to fault motion. The 1988 collapse is located north of the transpressive Relizane fault, which have slightly uplifted the southern side of the Ouarsenis Mountains with respect to the Chelif Basin. The deep voids near Boukadir town below 55 m south of the fault documented in boreholes (Fig. 8-A) and below 62 m north of the fault evidenced in the collapsed sinkhole could have been originally at the same level, and later vertically offset by fault motion. Their origin can be similar.

These deep cavities as well as the 1988 deep void are not inferred to have an hypogene origin. Indeed, the morphology of hypogenous caves is characterized by an absence of configuration with the topography (*Mylroie* et al., *2017*), and do not present either ponors or connections to the surface (*Osborne, 2017*). On the contrary, in Boukadir, the deep aquifer is directly connected to the outcropping carbonate platform (*Blanc, 1984*). Moreover, the presence of pollutant (e.g., nitrates) in the deep aquifer coming from agriculture is also a proof of this connection (*Bouchenouk, 2013*). Finally, the thick layer of Tortonian blue marls below the carbonates forms a thick impermeable barrier to deep hydrothermal waters preventing hypogenous processes.

Deep open cavities in Boukadir piedmont and the 1988 one must have developed in the vadose zone at the top of the aquifer where running water presents a velocity high enough to drain the insoluble minerals. These deep karstic levels took place when the water table was much lower than today, probably simultaneously with the deep cutting of the Taflout and Oued Sly Rivers (Fig. 8-A and 9). We infer that this lowstand is related to Messinian drop affecting the Mediterranean Sea level. The 1988 cavity is located north of the Relizane Fault Zone; the other close deep voids and the buried carbonate incision along rivers are located south of the Relizane Fault, and the low base level responsible for their common formation cannot be attributed to tectonics.

### 5.4. Synthesis model for the different karstification levels in the ouarsenis

We propose here a model to explain the different karstification levels in the Ouarsenis in relation with base-level changes affecting the Mediterranean area since the Messinian. This schematic evolution of the karst is summarized in Fig. 17. We use the sea level reconstruction of Mocochain et al. (2006a,b, 2009) affecting the Ardèche platform in Southern France. They highlight that since the Messinian, the most significant base-level drop was induced by the Messinian Salinity Crisis (MSC) from ~5.97 to 5.32 Ma (*Krijgsman* et al., *1999*; *Lozar* et al., *2018*; *Hoffmann* et al., *2020*; *Costa* et al., *2021*). During the MSC, the gateway between the Atlantic Ocean and the Mediterranean suddenly closed (*Hsü* et al., *1972*; *Audra* et al., *2004*). This triggered the most dramatic crisis the Mediterranean Sea has ever known: a sea level drop of about −1500 m (*Ryan, 1976*). Around the Mediterranean Sea, rivers strongly incised forming deep canyons to adapt to the base level fall (*Clauzon, 1982*; *Julian and Nicod, 1984*; *Bini, 1994*; *Bourillot* et al., *2010*; *Krijgsman* et al., *2018*). During MSC, Algerian rivers must have been strongly impacted by the sea level drop because the Algerian coastline is located near the steepest slopes of the Alboran Sea. According to Rubino et al. (2010), two river canyons formed, one related to Chelif River and the other one to the Algiers system. During the MSC, the Chelif Basin which was previously occupied by a marginal sea was disconnected from the Mediterranean Sea, and filled with gypsum rich sediments (*Roveri* et al., *2014*; *Naimi* et al., *2020*; *Moulana* et al., *2021*). The large deep underground voids along the southern margin of the Chelif Basin and the deep down cutting of the Messinian platform by the Taflout and Oued Sly Rivers are considered here to form during this low base level, like in other areas around the Mediterranean Sea (*Bini, 1994; Audra* et al., *2004; Mocochain et al., 2006a,b*, *2009*). In association with the low river base-level, a low karstic phreatic level developed during that time at similar elevation. We see this imprint in the Boukadir piedmont.

After the MSC, a transgression characterizing the beginning of Pliocene occurred (Mocochain et al., 2006a,b *2009*). The Chelif Basin was reconnected to the Mediterranean Sea allowing the deposition of more

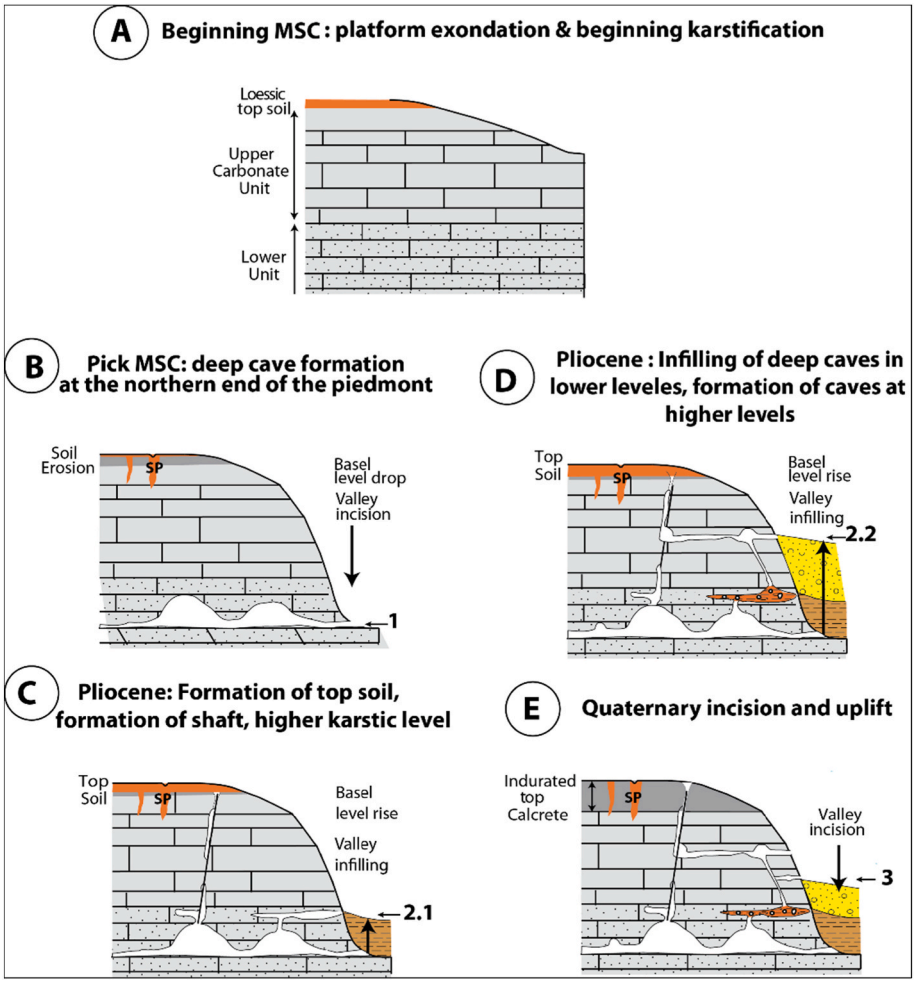


**Fig. 17.** Drawing of the northern piedmont of the Ouarsenis. 1. Valley incision during the Messinian Salinity Crisis (MSC) and development of deep cavities. 2. Valley aggradation, upper karstic network formation (e.g., chimney-shaft), soil development with solution piping and cavity partial cavity infill during the Pliocene transgression. 3. Quaternary incision due to a drop in the base level and uplift linked to the Relizane Fault. New karstic resurgence near the present base level is possible. SP: solution pipes.

than 1000 m of Zanclean marls with Mediterranean fauna (*Belhadji et al., 2008*; *Atif* et al. *2008*; *Arab* et al., *2015*). These transgressive marine clays are paired with thick deposits of Pliocene sandstones and conglomerates (gilbert delta) around the basin margins, and thus must have been associated with large river aggradation on the basin margins (*Rouchy* et al., *2007*; *Belhadji* et al., *2008*; *Atif* et al. *2008*; *Zhang and Jiang, 2011*; *Arab* et al., *2015*) (Fig. 17). This Pliocene river infilling is evidenced in the Taflout River whose valley was first filled by 35 m of clayey sediments, then by 30 m of Plio-Quaternary alluvium (Fig. 8-B). This base level rise would also have triggered a per ascensum adaptation of the Messinian karst drainages and the formation of a higher upper karstic phreatic level (Mocochain et al., 2006a,b, *2009*). Indeed, the lower part of the karstic network was completely drowned. Thus, water looking for an outlet is forced to flow up in chimney-shafts before creating a resurgence in the valley (*Mocochain et al., 2006a,b*). We observed such resurgence near Oued Rhiou and the Merdja (Fig. 15). In addition, the karstic network was partly infilled with fluvial processes. This mechanism would explain the infilling of red clay with carbonate gravels for the shallower kartic level evidenced in drillholes (Fig. 8-B). At that time, a paleosoil developed on the carbonate platform, which remains are visible at the southern extremity of the carbonate platform and in pipes in its central and northern parts. This paleosol favored the development of solution pipes.

Then, during the Quaternary, large variations in base level with a downward trend occurred linked to tectonic motion and to glacial-interglacial cycles (Mocochain et al., 2006a,b, *2009*). So, the aggradation should have mostly stopped except in tectonically subsiding basins. The tectonic uplift of the Carbonate Ouarsenis piedmont north of the Relizane Fault would have generated new downcutting of the rivers in several steps (Mocochain et al., 2006a,b). This mechanism would have stripped the sediments previously deposited in the valleys and at the top of the plarform, allowing the widespread outcropping of carbonates. The top soil remained only at the southern end of the platform. Calcrete development took place at its top as well as in the incising valleys. The progressive uplift would also have generated a deepening of the river base level and triggered the lowering of phreatic levels evidenced by the caves. This classical process can explain the occurrence of the Ghar Seffah and Ghar Zeboudja caves both located along the same river valley, the later on 450 m above the riverbed and the former one 530 m, as well as the Ghar Bou Baara located 173 m higher than the adjacent Oued Touchaït (Figs. 3 and 14 A and C). The stepped shelter cave morphology would also be related to river incision. However, the low phreatic level responsible for the deep void in relation with the Bir Djeneb is still debatable, and requires further investigation.

### 5.5. *Models for the two sinkholes associated with the boukadir carbonates*

There are two possible models for the formation of 1988 and Bir Djeneb sinkholes taking into account the characteristics of the karst presented. The first model is the case of a sinkhole formed in interaction with faults or factures and its interaction with a deep cave, also cut by this fault (SK1 model in Fig. 18 top). This is the classical formation of cavities in karstology. We infer that it is the case of the 1988 collapse sinkhole, located close to Relizane zone fault. The second model is the case of a collapse due to the emptying of a solution pipe crossing a deeper cave (SK2 model in Fig. 18 top). It may be the case of Bir Djeneb

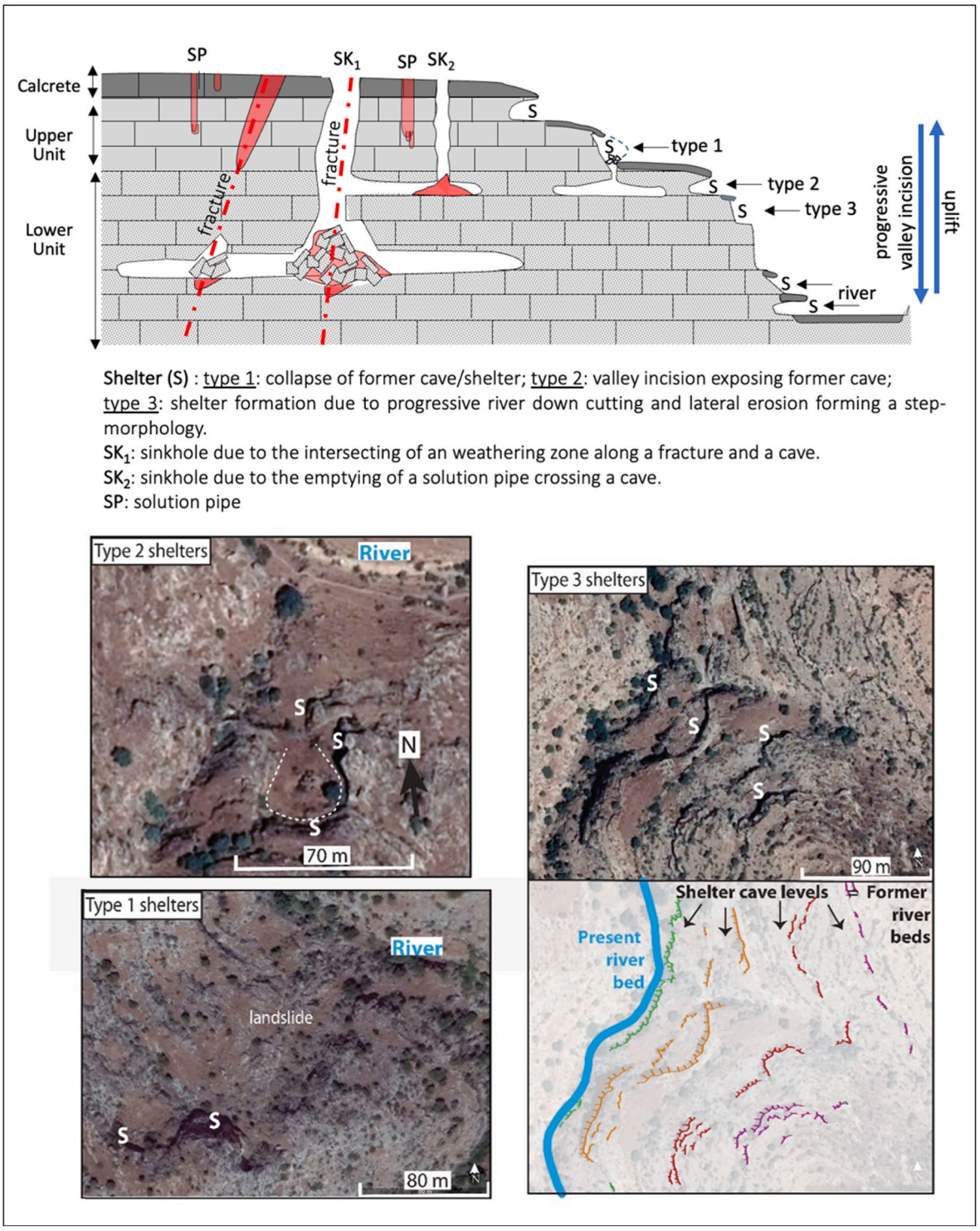


**Fig. 18.** Top: Drawing showing development processes of shelter caves in the carbonate Ouarsenis covered by a layer of calcrete. 1. Collapse of old caves. 2. Valley incision exposing former caves. 3. Formation of shelters due to the river incision by lateral erosion and slope retreat forming a stepped morphology. Differential weathering between different carbonate facies must also play a role. Bottom: Satellite images showing these processes in the field. The mapping of the different shelter caves illustrates the former riverbed position.

(Fig. 13-right). In that case, the pit attests to the development of an exokarst that intersects an older and deeper endokarst which could also have taken place during the Messinian Salinity Crisis.

## 6. Conclusion

Karst features in the Boukadir area are characterized by a low present-day activity related to low regional rainfall and the occurrence of a calcrete covering the carbonate range, which decreases the infiltration and increases surface runoff leading to a well-developed surface drainage. Frequent solution pipes and very well-developed fracturing network, parallel to the major Relizane Fault, are the main paths for infiltration. The solution pipe network was probably partly inherited from a period during which a top soil was covening the platform. In

addition, the carbonate facies (tufas) favour a diffuse infiltration, which reduced localized dissolution and flow at depth, and prevented the development of large caves. The endokarst is thus poorly developed and is represented by a few rare collapse sinkholes and a few caves, whereas the epikarst is prevalent and characterized by shelter caves with a complex origin, mainly related to the calcrete covering the carbonate platform at the surface. The regional uplift is a major control for the development of the shelter caves in association with progressive river incision. Finally, major deep paleokarst features were documented in the Boukadir piedmont close to the Relizane fault. The deepest karstic dissolution level is associated with paleo-river incisions, and thus attributed to the low base level during the Messinian Salinity Crisis (MSC). The MSC would thus be responsible for the large deep voids underlying the 1988 RN4 collapse as well as potentially the Bir Djeneb one. The following Pliocene aggradation buried all the MSC imprints filling the previous river incisions and flooding the MSC paleokarst. Beside this study that evidenced for the first time the imprint of the MSC low base level in Algeria, further researches are necessary to document and understand its extend and importance.

## Declaration of competing interest

The authors declare that they have no known competing financial interests or personal relationships that could have appeared to influence the work reported in this paper.

## Data availability

Data will be made available on request.

## Acknowledgments

The authors would like to thank Pr. Abdelhak BOUTALEB, director of the Laboratory of Metallogeny and Magmatism of Algeria (LMMA) FSTGAT – USTHB for his help and expertise especially in the field. We would also like to thank, Dr. Marthe LEFEVRE for her help, his proof-reading and these suggestions and Pr. Med Said GUETTOUCHE, director of the Geomorphology and Geohazards (G&G) Laboratory, FSTGAT – USTHB for his help, and also the colleagues who accompanied us in the field: Mr. Abdeldjalil GOUMRASSA, Mr. Sofiane MEDDANE and Mr. Badreddine MOULANA. Many thanks to Pr. André OZER and Dr. Alexandre PEETERS, for their contributions in the observation and analysis of aerial photographs. We are grateful to the speleologists of the Caving Club of Algiers for having accompanied us to the collapse sinkhole of Bir Djeneb, to the managers of the quarry of Oued Sly and to the gendarmerie of Boukadir town. A special thanks to Mr. Saber ABDELAZIZ, speleologist for the photos. We warmly thank the Bejaia, Chelif and Oran speleology club.

## Appendix. Coordinate of quarries boreholes and collapse sinkholes (WGS 84, UTM 31N)

| Nom | latitude | longitude | Source |
|---|---|---|---|
| RN4 collapse sinkhole | 36° 4′58.61"N | 1°10′2.24"E | LTPC (1989) |
| Bir Djeneb | 36° 1′2.97"N | 1° 6′35.37"E | Birebent (1947a) ANRH |
| Ghar Bou Baara | 36° 1′58.62"N | 1° 5′54.86"E | Birebent (1947a) ANRH |
| Ghar Seffah | 35°59′4.12"N | 1° 3′32.38"E | Birebent (1947a) ANRH |
| Ghar Zeboudja | 35°59′2.80"N | 1° 3′20.63"E | Birebent (1947a) ANRH |
| Oued Sly quarry | 36° 5′26.43"N | 1°14′8.33"E | Filled trip |
| Boukadir quarry | 36° 3′17.66"N | 1° 8′33.56"E | Filled trip |
| Sidi Abed quarry | 35°59′35.68"N | 1° 0′8.89"E | Filled trip |
| S1 drill core | 36° 4′53.06" | 1°10′19.92"E | LTCP |
| AEP Bouachria | 36°4′32.3739″ N | 1°10′15.0516″ E | BURGAP (2004) (ANRH) |
| Site Sonalgaz O. Sly | 36°5′18.9682″ N | 1°11′46.1326″ E | BURGAP (2004) (ANRH) |
| kh5 | 36° 2′40.72"N | 1° 5′36.58"E | BURGAP (2004) (ANRH) |
| kh6 | 36° 2′48.09"N | 1° 5′14.20"E | BURGAP (2004) (ANRH) |

Coordinate of quarries, boreholes and collapse (WGS 84, UTM 31N).

## References

Aïfa, T., Zaagane, M., 2015. Neotectonic deformation stages in the central Ouarsenis culminating zone, Northwestern Algeria. Arabian J. Geosci. 8 (5), 2667–2680.

Alexandersson, T., 1974. Carbonate cementation in coralline algal nodules in the Skagerrak, North Sea; biochemical precipitation in undersaturated waters. J. Sediment. Res. 44 (1), 7–26. https://doi.org/10.1306/74D72964-2B21-11D7-8648000102C1865D.

Arab, M., Bracene, R., Roure, F., Zazoun, R.S., Mahdjoub, Y., Badji, R., 2015. Source rocks and related petroleum systems of the Chelif Basin (western Tellian domain, north Algeria). Mar. Petrol. Geol. 64, 363–385. https://doi.org/10.1016/j.marpetgeo.2015.03.017.

Atif, K.F.T., Bessedik, M., Belkebir, L., Mansour, B., Saint Martin, J.P., 2008. Le passage Mio-Pliocène dans le bassin du Bas Chélif (Algérie). Biostratigraphie et paléoenvironnements. Geodiversitas 30 (1), 97–116.

Audra, P., Mocochain, L., Camus, H., Gilli, E., Clauzon, G., Bigot, J.Y., 2004. The effect of the messinian deep stage on karst development around the Mediterranean Sea. Examples from southern France. Geodin. Acta 17 (6), 389–400. https://doi.org/10.3166/ga.17.389-400.

Bakalowicz, M., 2018. Coastal Karst Groundwater in the Mediterranean: a resource to be preferably exploited onshore, not from karst submarine springs. Geosciences 8 (7), 258. https://doi.org/10.3390/geosciences8070258.

Ballais, J.L., Cohen, J., 1981. Intérêt morphogénétique et paléoclimatique des travertins des Aurès (Algérie). Actes du Colloque de l'Association des Géographes français : Formations carbonatées externes, tufs et travertins, Paris, pp. 37–44, 9 mai.

Beldjoudi, H., Delouis, B., Heddar, A., Nouar, O.B., Yelles-Chaouche, A., 2012. The Tadjena earthquake (Mw= 5.0) of December 16, 2006 in the Cheliff region (northern Algeria): waveform modelling, regional stresses, and relation with the Boukadir fault. Pure Appl. Geophys. 169 (4), 677–691. https://doi.org/10.1007/s00024-011-0337-8.

Belhadji, A., Belkebir, L., Saint Martin, J.P., Mansour, B., Bessedik, M., Conesa, G., 2008. Apports des foraminifères planctoniques à la biostratigraphie du Miocène supérieur et du Pliocène de Djebel Diss (bassin du Chélif, Algérie). Geodiversitas 30 (1), 79–96.

Besser, H., Dhaouadi, L., Hadji, R., Hamed, Y., Jemmali, H., 2021. Ecologic and economic perspectives for sustainable irrigated agriculture under arid climate conditions: an analysis based on environmental indicators for southern Tunisia. J. Afr. Earth Sci., 104134

Bettahar, N., 2012. Effect of the climate and soil characteristics on the nitrogen balance in the north of Algeria. Horticulture 1.

Bettahar, N., Kettab, A., Benamara, A., Douaoui, A., 2008. Effet des conditions pédoclimatiques sur le bilan d'azote. Cas de la vallée du moyen Cheliff Occidental. Algerian Journal Of Technology –AJOT, ISSN 111-357X, Number Special – An International Publication of Engineering Sciences 1, 441–447.

Bini, A., 1994. Rapports entre la karstification périméditerranéenne et la crise de salinité du Messinien. Karstologia 23, 33–53. https://doi.org/10.3406/karst.1994.2329.

Birebent, J., 1947a. Rapport de spéléologie de l'Algérie : Inventaire. 1er Décembre 1947. Agence National Ressources Hydrauliques (ANRH), p. 13.
Birebent, J., 1947b. Spéléologie & étude des puits de la région avoisinant le Merdja entre Inkermann & Charon (Département d'Oran et d'Alger). Agence National des Ressources hydrauliques, Alger, p. 17 le 28 Décembre 1947. Rapport.
Birebent, J., 1948. Explorations souterraines en Algérie. Campagne 1946—1947. Ann. Speleol. 3 (2), 8.
Blanc, P., 1984. Ressources en eau des calcaires à lithothamorium de la rive gauche de l'Oued Chélif (Algérie). Ingenieurs Archit. Suisses 110 (9), 129–132. https://doi.org/10.5169/seals-75297.
Bouchenouk, I., 2013. Processus d'enrichissement en nitrates des eaux souterraines dans les zones semi-arides, cas de la plaine de Boukadir (nord-ouest Algerien). Doctoral dissertation, univ oran 2.
Boulaine, J., 1957. Etude des sols des plaines du Cheliff. Thèse d'Etat de l'Université d'Alger, p. 582.
Bourillot, R., Vennin, E., Rouchy, J.M., Blanc-Valleron, M.M., Caruso, A., Durlet, C., 2010. The end of the Messinian salinity crisis in the western Mediterranean: insights from the carbonate platforms of south-eastern Spain. Sediment. Geol. 229 (4), 224–253. https://doi.org/10.1016/j.sedgeo.2010.06.010.
Brahmi, S., Baali, F., Hadji, R., Brahmi, S., Hamad, A., Rahal, O., Zerrouki, H., Saadali, B., Hamed, Y., 2021. Assessment of groundwater and soil pollution by leachate using electrical resistivity and induced polarization imaging survey, case of Tebessa municipal landfill, NE Algeria. Arabian J. Geosci. 14 (4), 1–13.
Brives, A., Ferrand, M., 1912. Carte géologique de l'Algérie 1:50,000: 105. Service géologique de l'Algérie, Alger.
BURGAP, 2004. Prospection géophysique à travers la région : HAMADNA - BOUKADIR. Wilaya de Relizane. Rapport définitif. Agence National Ressources Hydrauliques (ANRH), p. 57.
C.G.G, 1966. Etude Hydrologique par prospection électrique et sismique dans l'oued Sly.
Clauzon, G., 1982. Le canyon messinien du Rhône ; une preuve décisive du" desiccated deep-basin model" (Hsü, Cita et Ryan, 1973). Bull. Soc. Geol. Fr. 7 (3), 597–610.
Collignon, B., 1991. Les principaux karsts d'Algérie, Quelques éléments de synthèse, actes du 9ème Congrès National de la SSS. Nationalen kongresses der SHG. Akten des 9.
Collignon, B., 2022. Karsts et grottes d'Algérie. Les principales régions karstiques d'Algérie et leurs cavités le splus remarquables. geomorphology and environmental change. Karstologia Mémoires n°27-2022. Assossiation Française de Kartologie, p. 255.
Costa, G., Bavestrello, G., Cattaneo-Vietti, R., Pierre, F.D., Lozar, F., Natalicchio, M., Violanti, D., Pansini, M., Rosso, A., Bertolino, M., 2021. Palaeoenvironmental significance of sponge spicules in pre-Messinian crisis sediments, Northern Italy. Facies 67 (2), 1–21. https://doi.org/10.1007/s10347-020-00619-4.
Delattre, N., 1985. Les puits naturels du Tournaisis. Étude de leur localisation et contribution à l'étude de leur genèse. Ann. Soc. Geol. Belg. 108, 117–123.
Derder, M.E.M., Henry, B., Amenna, M., Bayou, B., Maouche, S., Besse, J., Abtout, A., Boukerbout, H., Bessedik, M., Bourouis, S., Ayache, M., 2011. Tectonic evolution of the active Chelif basin (northern Algeria) from paleomagnetic and magnetic fabric investigations. New Frontiers in Tectonic Research–At the Midst of Plate Convergence 3–26.
Derijcke, F., 1979. Le karst souterrain du Tournaisis, du Paléozoïque à aujourd'hui. Ann. Soc. Geol. Belg. 102, 27–30.
Ek, C., Mathieu, L., Lacroix, D., 1981. Croûtes et encroûtements calcaires en climat méditerranéen. L'exemple du bled Ouljamane (Maroc oriental). Actes du Colloque de l'Association des Géographes français : Formations carbonatées externes, tufs et travertins, vol. 3. Association française de Karstologie, mémoire, pp. 61–72.
Ek, C., 1976. Les phénomènes karstiques. In: Géomorphologie de la Belgique, Hommage au Professeur P. Macar, A. Pissart, éd. sc. Laboratoire de Géographie physique de l'Université de Liège, pp. 137–157, 224.
Ek, C., Jaspar, A., Michel, R., 1999. La cartographie des contraintes karstiques en Région wallonne (Belgique). Bulletin de la Société géographique de Liège 36, 53–64.
Ek, C., Michel, R., Mousny, V., Closson, D., 1997. Dynamics of the karstic features of Sprimont (Belgium) and its consequences on land use planning. Preliminary note. In: Proceedings of the 12th International Congress of Speleology, vol. 5. La-Chaux-de-Fonds, Switzerland, pp. 13–14.
Esteban, M., Klappa, C.F., 1983. Subaerial exposure environments. In: Shole, P.A., Bebout, D.G., Moore, C.H. (Eds.), Carbonate Depositional Environments. American Association of Petroleum Geologists. Memoir 33, pp. 1–54.
FAO, 1989. The State of Food and Agriculture, vol. 37. Food & Agriculture Organization of the UN (FAO).
Gocke, M., Pustovoytov, K., Kuzyakov, Y., 2012. Pedogenic carbonate formation: recrystallization versus migration—process rates and periods assessed by 14C labeling. Global Biogeochem. Cycles 26 (1). https://doi.org/10.1029/2010GB003871.
Goudie, A.S., 1983. Calcrete. In: Goudie, A.S., Pye, K. (Eds.), Chemical Sediments and Geomorphology. Academic Press, London, pp. 93–131.
Hamad, A., Abdeslam, I., Fehdi, C., Badreddine, S., Mokadem, N., Legrioui, R., Hadji, R., Hamed, Y., 2021. Vulnerability characterization for multi-carbonate aquifer systems in semiarid climate, case of Algerian–Tunisian transboundary basin. International Journal of Energy and Water Resources 1–14.
Hamed, Y., Hadji, R., Redhaounia, B., Zighmi, K., Bâali, F., El Gayar, A., 2018. Climate impact on surface and groundwater in North Africa: a global synthesis of findings and recommendations. Euro-Mediterranean Journal for Environmental Integration 3 (1), 25.
Harris, I., Osborn, T.J., Jones, P., Lister, D., 2020. Version 4 of the CRU TS monthly high-resolution gridded multivariate climate dataset. Sci. Data 7 (1), 1–18. https://doi.org/10.1038/s41597-020-0453-3.
Hoffmann, R., Bitner, M.A., Pisera, A., Jäger, M., Auer, G., Giraldo-Gómez, V., Kočí, T., Buckeridge, J., Mueller, M., Stevens, K., Schneider, S., 2020. Late Miocene biota from the Abad member of the carboneras-nijar basin (Spain, Andalusia): a bathyal fossil assemblage pre-dating the messinian salinity crisis. Geobios 59, 1–28. https://doi.org/10.1016/j.geobios.2020.03.002.
Hsü, K.J., Cita, M.B., Ryan, W.B.F., 1972. The origin of Mediterranean evaporites. In: Ryan, W.B.F., Hsu, K.J. (Eds.), Initial Rep. Deep Sea Drill. Proj. 13, 1203–1231.
Julian, M., Nicod, J., 1984. Paléokarsts et paléo-géomorphologie néogènes des Alpes Occidentales et régions adjacentes. Karstologia 4 (1), 11–18. https://doi.org/10.3406/karst.1984.939.
Kingumbi, A., Bargaoui, Z., Hubert, P., 2009. Investigations sur la variabilité pluviométrique en Tunisie centrale. J. Sci. Hydrol. 50, 493–508. https://doi.org/10.1623/hysj.50.3.493.65027.
Krijgsman, W., Capella, W., Simon, D., Hilgen, F.J., Kouwenhoven, T.J., Meijer, P.T., Sierro, F.J., Tulbure, M.A., van den Berg, B.C.J., van der Schee, M., Flecker, R., 2018. The Gibraltar corridor: watergate of the Messinian salinity crisis. Mar. Geol. 403, 238–246. https://doi.org/10.1016/j.margeo.2018.06.008.
Krijgsman, W., Hilgen, F.J., Raffi, I., Sierro, F.J., Wilson, D.S., 1999. Chronology, causes and progression of the Messinian salinity crisis. Nature 400 (6745), 652–655. https://doi.org/10.1038/23231.
Lipar, M., Webb, J.A., White, S.Q., Grimes, K.G., 2015. The genesis of solution pipes: evidence from the Middle–Late Pleistocene Bridgewater Formation calcarenite, southeastern Australia. Geomorphology 246, 90–103. https://doi.org/10.1016/j.geomorph.2015.06.013.
Lozar, F., Violanti, D., Bernardi, E., Dela Pierre, F., Natalicchio, M., 2018. Identifying the Onset of the Messinian Salinity Crisis: a Reassessment of the Biochronostratigraphic Tools (Piedmont Basin, NW Italy. https://doi.org/10.1127/nos/2017/0354.
LTPC, 1989. Collapse of the RN4 (Oued Sly. Boukadir). Center Public Works Laboratory, p. 58.
Mathieu, L., Lacroix, D., Ek, C., Rassel, A., 1983. Sols et croûtes calcaires dans la basse Moulouya intérieure. Recherches géographiques à Strasbourg, n° spécial 22–23, 97–109.
Mattauer, M., 1958. Étude géologique de l'Ouarsenis oriental. Bull. Serv. Carte Géol. Alger. (Nouvelle Séries) 17, 1–534.
Meddi, H., Meddi, M., Assani, A.A., 2014. Study of drought in seven Algerian plains. Arabian J. Sci. Eng. 39, 339–359. https://doi.org/10.1007/s13369-013-0827-3.
Meghraoui, M., 1988. Géologie des zones sismiques du Nord de l'Algérie : Paléosismologie, tectonique active et synthèse sismotectonique thèse d'État. université Paris- 11, 356.
Meghraoui, M., Cisternas, A., Philip, H., 1986. Seismotectonics of the lower Cheliff basin: structural background of the El Asnam (Algeria) earthquake. Tectonics 5 (6), 809–836.
Meghraoui, M., Morel, J.L., Andrieux, J., Dahmani, M., 1996. Tectonique plio-quaternaire de la chaine tello-rifaine et de la mer d'Alboran ; une zone complexe de convergence continent-continent. Bull. Soc. Geol. Fr. 167 (1), 141–157.
Mocochain, L., Audra, P., Clauzon, G., Bellier, O., Bigot, J.Y., Parize, O., Monteil, P., 2009. The effect of river dynamics induced by the Messinian Salinity Crisis on karst landscape and caves: example of the Lower Ardèche river (mid Rhône valley). Geomorphology. https://doi.org/10.1016/j.geomorph.2008.09.021.
Mocochain, L., Bigot, J.Y., Clauzon, G., Faverjon, M., Brunet, P., 2006a. La grotte de Saint-Marcel (Ardèche): un référentiel pour l'évolution des endokarsts méditerranéens depuis 6 Ma. Karstologia 48 (1), 33–50.
Mocochain, L., Clauzon, G., Bigot, J.Y., 2006b. Réponses de l'endokarst ardéchois aux variations eustatiques générées par la crise de salinité messinienne. Bull. Soc. Géol. France 177 (1), 27–36.
Mouici, R., Baali, F., Hadji, R., Boubaya, D., Audra, P., Fehdi, C.É., et al., 2017. Geophysical, Geotechnical, and Speleologic assessment for karst-sinkhole collapse genesis in Cheria plateau (NE Algeria). Min. Sci. 24, 59–71.
Moulana, M.L., Hubert-Ferrari, A., Guendouz, M., El Ouahabi, M., Boutaleb, A., Boulvain, F., 2021. Contribution to the sedimentology of the messinian limestones of Boukadir (Chelif 2 basin-Algeria). Geol. Belg. https://doi.org/10.20341/gb.2021.002.
Moulana, M.L., 2022. Le Miocène post-nappe de la vallée du Chélif. In: book: Karsts et grottes d'Algérie. Les principales régions karstiques d'Algérie et leurs cavités le splus remarquables. geomorphology and environmental change. Assossiation Française de Kartologie, pp. 94–98 (Chapter 7): Le Tell Oranais. Karstologia Mémoires n°27-2022.
Mylroie, J., Mylroie, J., Humphreys, W., Brooks, D., Middleton, G., 2017. Flank margin cave development and tectonic uplift, Cape Range, Australia. J. Cave Karst Stud. 79 (1), 35–47. https://doi.org/10.4311/2015ES0142.
Naimi, M.N., Mansour, B., Cherif, A., 2020. First record of the Halimeda-rich beds from the Tessala–beni chougrane messinian carbonate platform (lower Chelif Basin, NW Algeria). In: Conference : GeoConvention 2020. At : Calgary, Canada, p. 5.
Ncibi, K., Hadji, R., Hajji, S., Besser, H., Hajlaoui, H., Hamad, A., Mokadem, N., Ben Saad, A., Hamd, M., Hamed, Y., 2021. Spatial Variation of Groundwater Vulnerability to Nitrate Pollution under Excessive Fertilization Using Index Overlay Method in Central Tunisia (Sidi Bouzid Basin). Irrigation and Drainage.
Nekkoub, A., Baali, F., Hadji, R., Hamed, Y., 2020. The EPIK multi-attribute method for intrinsic vulnerability assessment of karstic aquifer under semi-arid climatic conditions, case of Cheria Plateau, NE Algeria. Arabian J. Geosci. 13 (15), 1–15.
Neurdin-Trescartes, J., 1992. Le remplissage sédimentaire du bassin néogène du Chelif, modèle de référence de bassins intramontagneux. Thèse de Doctorat es Science, université de Pau et pays de l'Adour, France, p. 332.
Osborne, A., 2017. Eastern Australian karsts and caves are different. J. Cave Karst Stud. 79 (1), 48–52.
Ourabia, K., Benallal, K., 1989. Report of the Collapse of RN4, vols. 1–3. Central Laboratory of Public Works, p. 7.

Penman, H.L., 1948. Natural evaporation from open water, bare soil and grass. Proc. Roy. Soc. Lond. 193, 120–145. https://doi.org/10.1098/rspa.1948.0037.
Perrodon, A., 1957. Etude géologique des bassins néogènes sublittoraux de l'Algérie occidentale (Doctoral dissertation), Serv. Carte Géol. Algérie 12, 328 n.s.
Rouchy, J.M., Caruso, A., Pierre, C., Blanc-Valleron, M.M., Bassetti, M.A., 2007. The end of the Messinian salinity crisis: evidence from the Chelif Basin (Algeria). Palaeogeogr. Palaeoclimatol. Palaeoecol. 254 (3–4), 386–417. https://doi.org/10.1016/j.palaeo.2007.06.015.
Roveri, M., Flecker, R., Krijgsman, W., Lofi, J., Lugli, S., Manzi, V., Sierro, F.J., Bertini, A., Camerlenghi, A., De Langj, G., Govers, R., Hilgen, F.J., Hübscher, C., Meijer, P.Th, Stoica, M., 2014. The Messinian Salinity Crisis: past and future of a great challenge for marine sciences. Mar. Geol. 352, 25–58. https://doi.org/10.1016/j.margeo.2014.02.002.
Rubino, J.L., Haddadi, N., Camy-Peyret, J., Clauzon, G., Suc, J.P., Ferry, S., Gorini, C., 2010. Messinian salinity crisis expression along North African margin. In: North Africa Technical Conference and Exhibition. Society of Petroleum Engineers. https://doi.org/10.2118/129526-MS.
Ryan, W.B., 1976. Quantitative evaluation of the depth of the western Mediterranean before, during and after the Late Miocene salinity crisis. Sedimentology 23 (6), 791–813. https://doi.org/10.1111/j.1365-3091.1976.tb00109.x.
Salem, B.B., 1989. Arid Zone Forestry: a Guide for Field Technicians. FAO Conservation Guide. No.20 pp.vii + 143 pp. ref.8 pp.
Scet – Argi, 1985. Hydrologie - Hydrogéologie et bilan des ressources, Etude du réaménagement et de l'extension du périmètre du moyen Chéliff : Rap A1.1. 2. Pub. Ministère de l'Hydraulique, p. 72.
Sebbar, A., Badri, W., Fougrach, H., Hsain, M., Saloui, A., 2011. Study of the variability of the rainfall regime in northern Morocco (1935-2004). Drought 22 (3), 139–148.
Tighilt, F.A., 1990. L'effondrement de Boukadir (Bas Chelif Oriental): Causes géologiques et risque lié à ce phénomène. Thèse de Doctorat, université des Sciences et de la Technologie Houari Boumedienne, USTHB.
Willems, L., Rodet, J., 2018. Karst and underground landscapes in the cretaceous chalk and calcarenite of the Belgian-Dutch border—the montagne saint-Pierre. In: Landscapes and Landforms of Belgium and Luxembourg. Springer, Cham, pp. 177–192.
Willems, L., Rodet, J., Fournier, M., Laignel, B., Dusar, M., Lagrou, D., Pouclet, A., Massei, N., Dussart-Baptista, L., Compère, Ph, Ek, C., 2007. Polyphase karst system in Cretaceous chalk and calcarenite of the Belgian-Dutch border. Zeitschrift fur Geomorphologie 51 (3), 361–376. https://doi.org/10.1007/978-3-319-58239-9_11.
Woodward, J.C., Lewin, J., 2009. Karst geomorphology and environmental change. In: The Physical Geography of the Mediterranean. Oxford University Press, pp. 287–317. https://doi.org/10.1093/oso/9780199268030.003.0022.
Wright, V.P., Tucker, M.E., 1991. Calcretes: an introduction. In: Wright, V.P., Tucker, M. E. (Eds.), Calcretes. IAS Reprint Series, vol. 2. Blackwell Scientific Publications, Oxford, pp. 1–22.
Yacono, X., 1955. Colonisation des plaines du Chéliff (de Lavigerie au confluent de la Mina). Tome 1, Imprimerie Imbert, Alger.
Yelles-Chaouche, A., Boudiaf, A., Djellit, H., Bracene, R., 2006. La tectonique active de la région nord-algérienne. Compt. Rendus Geosci. 338 (1–2), 126–139. https://doi.org/10.1016/j.crte.2005.11.002.
Zhang, Y., Jiang, Z., 2011. Outcrop characterization of an early Miocene slope fan system, Chelif Basin, Algeria. Energy Explor. Exploit. 29 (5), 633–646. https://doi.org/10.1260/0144-5987.29.5.633.